Spectroscopic Analysis of Solar and Cosmic X-Ray Spectra

I. The Nature of Cosmic X-Ray Spectra and Proposed Analytical Techniques

by

A.B.C. Walker, Jr.

National Aeronautics and Space Administration
Grant NSG-7099

and

National Aeronautics and Space Administration
Ames Research Center Grant NSG-2049

SUIPR Report No. 628

May 1975

INSTITUTE FOR PLASMA RESEARCH
STANFORD UNIVERSITY, STANFORD, CALIFORNIA

SPECTROSCOPIC ANALYSIS OF SOLAR AND COSMIC X-RAY SPECTRA

I. The Nature of Cosmic X-Ray Spectra and Proposed Analytical Techniques*

A.B.C. Walker, Jr.
Institute for Plasma Research and
Department of Applied Physics
Stanford University
Stanford, California 94305 USA

Invited Paper Presented at the Symposium on the
"Techniques of Solar and Cosmic X-Ray Spectroscopy"
Mullard Space Science Laboratories
Holmbury St. Mary, Surrey, England
May 22-23, 1975

To be published in Space Science Instrumentation

*The work presented in this paper was supported by NASA Grant NSG-7099 and NASA-Ames Grant NSG-2049.

ABSTRACT

The interpretation of high resolution x-ray spectra of the solar corona has established the structure and composition of the corona. We present a brief review of the techniques developed in the study of the temperature and density structure and composition of the corona, as an introduction to a discussion of the modifications in these techniques which will be required for the study of cosmic sources, and a specification of the type of observation which will be required for the spectroscopic study of these sources.

Two major programs of spectroscopic observations of cosmic sources are discussed: the study of the spectra of individual sources, and the study of the interstellar medium (ISM) by the analysis of its effect on the spectra of selected individual sources whose intrinsic spectra can be inferred by other techniques. We first discuss the effect of structure within the ISM, including the presence of interstellar grains, the ionization structure, the presence of molecules, and the development of more sophisticated models of the opacity of the ISM which take account of this structure. We then review the expected spectral structure of individual cosmic sources, with emphasis on the galactic supernovae remnants and the galactic binary x-ray sources. The observational and analytical requirements imposed by the characteristics of these individual sources will be identified, and the prospects for the analysis of abundances, and the prospects for the study of the physical parameters within these objects will be assessed. Prospects for the spectroscopic study of other classes of observed and predicted cosmic x-ray sources, such as the extended regions of soft emission within the galaxy, the extragalactic Abell cluster sources, and the coronae of late type main sequence and giant stars will be briefly discussed.

TABLE OF CONTENTS

I. INTRODUCTION

Spectroscopic techniques have been extensively used in the analysis of the euv and x-ray spectrum of the solar corona. Observations of cosmic x-ray sources at low resolution are now sufficiently well advanced that detailed predictions of the spectral characteristics which high resolution observations may be expected to reveal can be made. For at least one class of galactic x-ray source, the supernovae remnants, an emission line spectrum characteristic of a low density Maxwellian plasma, similar to the solar spectrum, is expected. For the class of binary galactic x-ray sources, the x-ray flux is generated in an optically thick atmosphere, and spectral features will be significantly broadened by Thomson scattering and resonance scattering; the analysis of the weak line cores which should ultimately be observable will be substantially different from the solar case. However, photoionization processes in the extended atmosphere which surrounds the compact object in these sources, and in the atmosphere of the normal companion, may result in strong emission and absorption features in the spectra of these sources. In the present paper we briefly review the spectroscopic techniques which have been used in the analysis of solar observations and discuss the modifications which must be made in order to apply these techniques to cosmic x-ray spectra.

The x-ray opacity of the interstellar medium is important in two ways; it determines the wavelength range in which objects at various distances can be observed, and the detailed dependence of the x-ray opacity on wavelength contains information on interstellar abundances and ionization structure, and the composition and size of the interstellar grains. A detailed model of the x-ray opacity in the direction of the

Crab nebula is discussed to illustrate the effect of structure in the interstellar medium on x-ray absorption. Observations of the density in the interstellar medium in the vicinity of the earth are also reviewed, and the implications of these observations for the study of soft x-ray sources, such as the coronae of normal stars, are discussed.

The prospect for the observation of the coronae of nearby late type stellar dwarfs and giants appears to be excellent. Recent ultraviolet observations of stellar coronae are discussed, and model calculations of the expected fluxes are presented. For nearby objects, it would appear to be feasible to carry out observations to 304Å and beyond, and many diagnostic techniques developed for coronal studies will be useful for this special class of object.

II. REVIEW OF SPECTROSCOPIC STUDIES OF THE SOLAR CORONA

The analysis of the structure of the corona with spectroscopic observations has been carried out using two different approaches. Pottasch [1,2] has developed a technique which makes use of the observed emission in the resonance lines of a large number of ions whose emission is peaked over relatively narrow temperature intervals within the range of temperatures, $\sim 10^5 - 2 \times 10^6$ °K, which are important within the solar transition region and low corona. Pottasch was able to invert the emission integral, after making the assumption that the solar emission measure function varies slowly over the temperature range within which each ion is efficiently excited. If a sufficiently large number of ions are included in the analysis, it is possible to obtain an emission measure function for the ions of each element, and consequently relative abundances as well as the thermal structure may be obtained. The second approach has made use of selected line ratios for transitions within the same ion which are particularly sensitive to either density or temperature. The analysis of this type of observation has generally made the assumption that the coronal structures which have been observed are isothermal (or isobaric); however, this restriction is not essential to the analysis. In this section I review the techniques which have been developed for the analysis of the structure of the corona. General reviews of spectroscopic techniques have been written by Gabriel and Jordan [3] and by Walker [4,5].

The calculation of the excitation function of lines, and of the x-ray continuum is central to the analysis of spectroscopic observations. Walker [4,5] and Gabriel and Jordan [3] have reviewed the

calculation of these excitation functions. The coronal calculations may be applied directly to the emission spectra of supernovae remnants (SNR's). However, the emission function will have a quite different form for the optically thick binary x-ray sources. The emission function for these sources is discussed in more depth in a later section.

II.A THE DEVELOPMENT OF THERMAL MODELS

Jefferies, Orrall and Zirker [6] have developed a general method for the analysis of line emission from an optically thin gas. Using the formalism developed by Jefferies et al. the flux in a coronal line may be written [7]

$$F_{Zzij} = a_H A_Z \iint dS \int dT_e M(T_e, G_k) a_z(T_e) J_{ij}(T_e) \quad . \qquad (1)$$

where $i \rightarrow j$ refers to a specific transition from upper level i to lower level j in ionization stage z of element Z with relative abundance A_Z. The fractional abundance of ionization stage z is $a_z(T_e)$, and $J_{ij}(T_e, n_e)$ is peculiar to each transition and depends only on atomic parameters. For resonance transitions J_{ij} is, to the first approximation, equal to the product of the collisional excitation rate into the level i, and the branching ratio for the transition $i \rightarrow j$. The integral is carried over the area $S(x_1, x_2)$ which is unresolved in the observational data to be analyzed, and x_1 and x_2 are coordinates orthogonal to the line of sight. The emission measure, $M(T_e, G_k)$, is defined by a set of parameters G_k.

Implicit in this approach is the assumption of a functional relationship between temperature and density, viz

$$n_e = n_e(T_e) \quad .$$

The original analysis of Pottasch did not make any assumptions regarding the physical model of the transition region, and so derived a general emission measure function and a set of relative abundances, i.e. in equation (1) both the constants G_k which define the emission measure function and the relative abundances A_Z of the elements whose lines are used in the analysis are regarded as parameters. Pottasch's technique has been extended to coronal lines by a number of experimenters [4,7,8,9,10,11,12,13]. Figure 1 illustrates a typical coronal model derived using the basic Pottasch technique. As we shall discuss in Section 4, the development of this type of model is a realistic goal for the strongest supernovae remnants.

The availability of spatially resolved observations of the solar corona has led to the development of more detailed models of coronal structure, and the imposition of restrictions on the coronal distribution function. Dupree [14] has developed a model in which it is assumed that the transition region is isobaric

$$P = n_e T_e = \text{const.}$$

and that the conductive flux in the transition region

$$f = \kappa T^{5/2} (dT/dh)$$

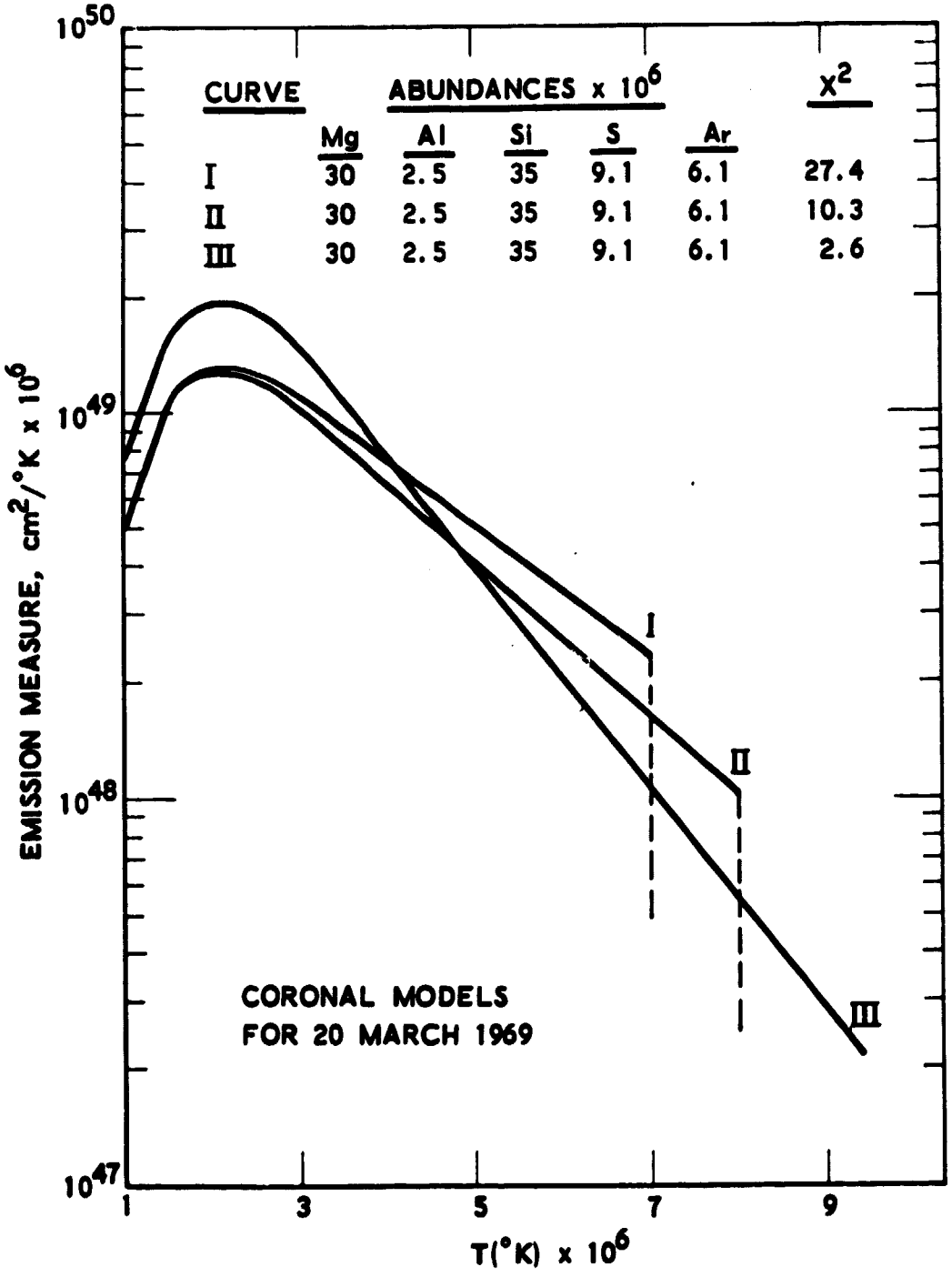

Figure 1. Models of the Coronal Emission Measure (after Walker et al., Ref. 7)

is also a constant. The thermal conductivity is given by K, and h is the height in the (assumed) spherically symmetric atmosphere. Kopp [15] and Pneuman [16] have developed more sophisticated models in which the effect of the magnetic field is taken into account by making the assumption

$$p + B^2/8\pi = \text{const.}$$

Jordan [17] has developed models which make explicit use of the fact that the high thermal conductivity in the direction of the magnetic field results in coronal structures which tend to be isothermal along the field lines, with the largest thermal gradients across field lines.

In the preceding discussion, no attempt has been made to make use of the enhanced sensitivity of particular line ratios to the physical parameters of the coronal plasma, such as temperature, density, or the relative abundance of a particular pair of elements. Such "diagnostic" line pairs are extremely useful because we can often determine, with their use, a particular physical parameter of the plasma without the construction of a complete model of the atmosphere. These determinations are possible because the line ratios involved depend only weakly on the configuration of the solar atmosphere, and allow conclusions to be drawn about coronal properties which are independent of the special set of assumptions which are implicit in a particular model.

II.B SPECTROSCOPIC TECHNIQUES FOR THE STUDY OF TEMPERATURE

The line ratios used for temperature diagnostics involve the ratio of two lines which depend on the population of a single ionization stage, but which have excitation functions which depend on temperature in different ways. Three techniques have been used:

1. The relative intensity of the 2s - 2p and 2s - 3p lines of lithium-like ions is temperature sensitive because of the large energy difference of the two transitions.

2. The relative intensity of two lines in the same series, such as the ratio Lyman-α/Lyman-β is temperature sensitive over a limited range of temperatures.

3. The intensity of satellite lines, which are formed by recombination processes, has a different temperature dependence from that of resonance lines which are collisionally excited.

Malinovsky and Heroux [18] have analyzed the relative intensities of the 2s - 2p and 2s - 3p lines of O VI, Ne VIII, and Mg X in the corona, finding good agreement with the theoretical intensity ratios provided a thermal model of the transition region is used to interpret the observations. Unfortunately, this technique is not suitable for the analysis of most cosmic x-ray sources since the 2s - 2p lines of all abundant lithium-like ions are not transmitted by the interstellar medium.

Rugge and Walker [19] have analyzed the relative intensities of the Lymna-α and Lyman-β lines of O VIII, Mg XII, and Si XIV, using the theoretical line ratios calculated by Hutcheon and McWhirter [20]. The availability of a coronal model allowed a detailed comparison for the O VIII lines, and excellent agreement with the theory was found. This technique should be useful for the study of cosmic sources since the Lyman lines of O, Ne, Mg, Si, and S should be observable for the most intense supernovae remnants.

The relative intensity of satellite and resonance lines varies as [21]

$$I_S/I_R \sim T^{-1}$$

Gabriel [21], Parkinson [22], and Walker and Rugge [23] have used the relative intensities of satellite and resonance lines to determine coronal temperatures. The relative intensity of the satellite lines increases as Z increases along a given isoelectronic sequence. For helium-like ions the strongest and most easily resolved lithium-like satellite [Table I], $1s^2 2s\ ^2S - 1s2s2p\ ^2P$, is $\approx$ 15% as intense as the resonance line for Si XIII. The atomic rate constants which are required for the calculation of the intensity of the lithium-like satellite lines have been calculated by Gabriel [21] and by Bhalla, Gabriel and Presnyakov [21].

TABLE I

SATELLITE LINES FOR TEMPERATURE DETERMINATION

Ion	Resonance Line*	Satellite Line**	Temperature Range
O VII	21.602Å	22.020Å	$1.5 - 4 \times 10^6$
Ne IX	13.450Å	13.650Å	$2.5 - 6 \times 10^6$
Mg XI	9.168Å	9.285Å	$3 - 8 \times 10^6$
Si XIII	6.647Å	6.719Å	$6 - 14 \times 10^6$
S XV	5.038Å	5.086Å	$8 - 20 \times 10^6$
Fe XXV	1.850Å	1.862Å	$18 - 40 \times 10^6$

*$1s^2\ ^1S - 1s2p\ ^1P$

**$1s^2 2s\ ^2S - 1s2s2p\ ^2P$

II.C SPECTROSCOPIC TECHNIQUES FOR THE STUDY OF DENSITY

The density dependence of coronal emission lines can come about in two way,

1. An excited metastable level may be collisionally transferred to an adjacent excited level which has a faster radiative decay rate. The relative intensity of the lines from these coupled levels will be a sensitive function of density over some range of densities.

2. If an ion has multiplet structure within its ground level, or a low lying excited state which is metastable, the relative population of these levels can become density dependent. The relative intensity of lines whose upper levels are more efficiently excited from the ground level or from the low lying excited level will be density sensitive over some range of densities.

A large number of line pairs have been used for density studies in the corona, however relatively few of these lines are below $\sim$ 100Å, in the region where they can be observed for most cosmic x-ray sources.

The relative intensity of the helium-like lines from the $1s2p\ ^1P$, ^3P and $1s2s\ ^3S$ lines has been discussed by Gabriel and Jordan [3,24] and Mewe and Schrijver [25]. The relative intensity of these lines is shown in Figure 2. The range over which these lines are useful for density measurements is shown in Table II. Solar observations of the intensity ratio $I(2^3S - 1^1S)/I(2^3P - 1^1S)$ have so far resulted only in the establishment of upper limits to coronal densities. These observations are reviewed by Walker [5].

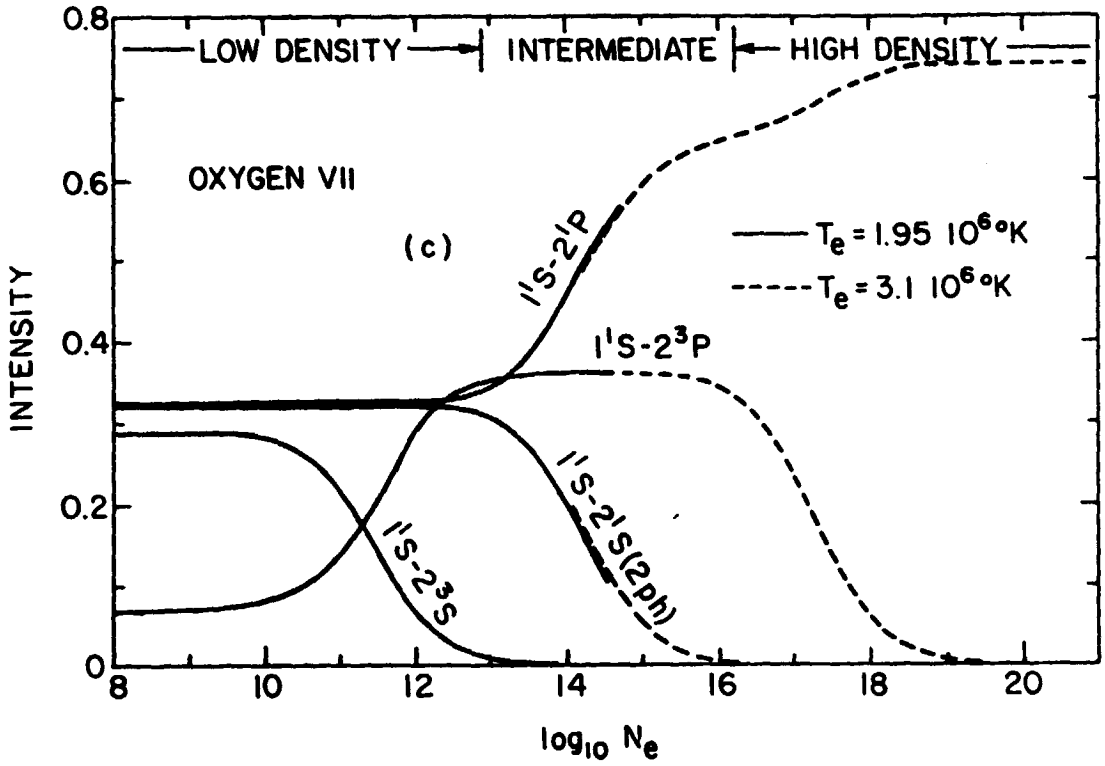

Fig. 2. Relative intensity of the lines (the 2^1S level decays by the emission of two photons) of the helium-like ion O VII as a function of density. (After Gabriel and Jordan, Ref. 3)

TABLE II

DENSITY SENSITIVE LINE RATIOS

SEQUENCE	TRANSITION	ION	WAVELENGTH (Å)	RANGE OF SENSITIVITY (cm^{-3})
He	$I(2^3S - 1^1S)/I(2^3P - 1^1S)$	C V	41.47/40.73	$5 \times 10^8 - 2 \times 10^{11}$
		O VII	22.10/21.80	$10^{10} - 5 \times 10^{12}$
		Ne IX	13.70/13.55	$1.5 \times 10^{11} - 10^{14}$
		Mg XI	9.31/9.23	$1.8 \times 10^{12} - 10^{15}$
		Si XIII	6.74/6.69	$1.5 \times 10^{13} - 10^{16}$
		S XV	5.10/5.07	$10^{14} - 5 \times 10^{16}$
		Fe XXV	1.87/1.86	$5 \times 10^{16} - 2 \times 10^{18}$
Be	$\frac{I(2s2p\ ^3P - 2s3d\ ^3D)}{I(2s^2\ ^1S - 2s3s\ ^1S)}$	Ne VII	106.2/127.65	$\sim 10^6 - 10^{13}$
		Mg IX	67.24/77.74	$\sim 10^7 - 10^{14}$
		Si XI	46.40/52.30	$\sim 5 \times 10^7 - 10^{15}$
		S XIII	33.95/37.60	$\sim 5 \times 10^8 - 10^{16}$
		Fe XXIII	~ 11.7/~ 13.0	$\sim 10^{10} - 10^{17}$
He	$I(2^3P - 1^1S)/I(2^1P - 1^1S)$	C V	40.73/40.27	$10^{12} - 10^{16}$
		O VII	21.80/21.60	$10^{13} - 10^{18}$
		Ne IX	13.55/13.45	$10^{14} - 10^{19}$
		Mg IX	9.23/9.17	$10^{15} - 10^{19}$
		Si XIII	6.69/6.65	$10^{16} - 10^{20}$
		S XV	5.07/5.04	$5 \times 10^{16} - 10^{21}$
		Fe XXV	1.86/1.85	$2 \times 10^{18} - 5 \times 10^{22}$
Ne	$I(3^3P_2 - 2^1S_0)/I(3^3P_1 - 2^1S_0)$	Fe XVII	17.10/17.05	$\geq 10^{13}$

The relative intensity of the lines excited from the ground level ($2s^2\ ^1S$) and from the metastable low lying $2s2p\ ^3P$ level of beryllium-like ions has been successfully used as a diagnostic technique in the solar corona [3,25,26,27,28,29,30]. These lines can be used as diagnostic tools over the range of densities from $\sim 10^5 - 10^{16}$ cm^{-3}, which covers the full range of densities found in the corona. Some problems remain in the interpretation of the observational results at this time due to uncertainties in some of the atomic rate constants required in the interpretation [30,31].

The lines of the transitions used for coronal diagnostics are at wavelengths which are unobservable except for the nearest cosmic x-ray sources. However, the $\Delta n = 1$ transitions in beryllium-like ions excited from the $2s^2\ ^1S$ and $2s2p\ ^3P$ levels will share the density sensitive nature of the $\Delta n = 0$ transitions. The lines of Mg IX, Si XI, S XIII, and Fe XXIII may be observable for a significant number of cosmic sources. The line ratio $I(2s2p\ ^3P - 2s3d\ ^3D)/I(2s^2\ ^1S - 2s3s\ ^1S)$ should be a good choice for observation since both lines have strong excitation cross-sections, and have already been observed in the corona for Ne VII, Mg IX and Si XI [18,32]. The range of densities over which these lines can be used for density diagnostics is given in Table II.

A final potentially density sensitive line in the x-ray region is the $2s^2 2p^6\ ^1S - 2s^2 2p^5 3s\ ^3P_2$ transition in Fe XVII, which has been resolved from the nearby $2s^2 2p^6\ ^1S - 2s^2 2p^5 3s\ ^3P_1$ line in the corona by Parkinson [13,33] and by Walker, Rugge and Weiss [11]. The lifetime of the $^3P_2$ level, which decays by a quadrapole transition is $\sim 2 \times 10^{-6}$ sec [34] and collisional coupling should affect the population of the $^3P_2$ and $^3P_1$ levels at densities near $\sim 10^{13}$ cm^{-3}. These strong lines may well be observable in the spectra of certain x-ray binary sources.

II.D TECHNIQUES FOR THE DETERMINATION OF RELATIVE ABUNDANCES

As pointed out in the introduction to this section, coronal abundances have been derived in the process of developing thermal models of the corona, using the lines from a large number of ions. Walker [5] has reviewed these abundance studies. Using x-ray observations alone this process has some limitations, since only 1 or 2 stages of ionization of a particular element may be observed in many cases. It is desirable, therefore, to develop diagnostic techniques for the determination of abundance which may be used without constructing a complete thermal model. The basic technique which has been employed is the analysis of the relative intensity of a pair of lines whose relative intensities are only weakly dependent on temperature, at least for a limited range of temperatures. Acton, Catura and Joki [35] have recently analyzed the observed relative intensity of the resonance lines of O VII and Ne IX, which is approximately constant (to a factor of $\sim$ 2-3) over the temperature range at which these lines are excited in the corona to obtain an O/Ne abundance ratio, without the use of a complete thermal model. More recently H.R. Rugge and the author [36] have studied the relative intensity of the resonance lines of Ne X and Mg XI. The relative intensity of these lines varies by less than $\pm$ 20% over the temperature range from $\sim 3 - 10 \times 10^6$ ^{o}K.

The analysis of a set of carefully selected line pairs can provide an initial set of relative abundances for the study of an astrophysical plasma of unknown composition such as the interstellar shock wave formed by a young supernovae remnant. These initial relative abundances may then be refined by the development of a complete thermal model with the use of equation (1).

II.E TECHNIQUES FOR THE STUDY OF THE IONIZATION EQUILIBRIUM

The astrophysical plasmas of interest in x-ray astronomy are not in local thermodynamic equilibrium (LTE). For a low density plasma in a dilute radiation field, the ionization balance is determined by the detailed balance between microscopic atomic processes. If the ionization balance is not changing with time, the plasma is presumed to be in "thermal equilibrium", however this situation is not to be confused with LTE. For a low density plasma in thermal equilibrium, the ionization equilibrium depends mainly on temperature, with a weak dependence on density only if $n_e \geq 10^{10}$ cm^{-3} [37-40]. The solar corona generally satisfies these conditions, and the preceding discussion has implicitly assumed that the astrophysical plasmas of interest are in thermal equilibrium. For a transient plasma, it may be necessary to describe the situation by three parameters: the electron temperature, T_e, the ion temperature, T_i, and an ionization temperature, T_z, which may vary from element to element [41]. Techniques for the study of the ionization equilibrium of low density plasmas make use of the relative intensity of spectral features which are formed primarily by collisional processes, and those which are formed by recombination processes, since these relative intensities are related to the relative populations of successive stages of ionization. An example of this type of observation is the relative intensity of the recombination edge for a particular ion, and the intensity of resonance lines for that ion. For example, the recombination edge for recombinations from O IX to O VIII is at 14.228Å, and the resonance line of O VIII is at 18.691Å. Observation of these features should prove feasible for objects such as young supernovae remnants, for which conditions of transient ionization may

persist for $\sim 10^{10}$ sec ($\sim$ 300 years). [A more complete discussion of supernovae remnants is presented in Section IV.] A second technique is the observation of two lines with upper levels of nearly identical excitation energy, from successive stages of ionization. An example of this approach is discussed by Gabriel [21], who has pointed out that the non-autoionizing satellite lines to the He-like ions will be formed by inner shell excitation in lithium-like ions, while the helium-like resonance lines are formed by excitation in the helium-like ions. Gabriel has used the relative intensity of the non-autoionizing $^2P - {}^4P$ (λ6.788) satellite line of Si XII, and of the Si XIII resonance line (λ6.646) to determine the ionization temperature of silicon ions in the corona shortly after a flare.

The ionization equilibrium calculations which have been used for coronal studies have assumed that the radiation field is sufficiently dilute that it does not affect ionization or recombination rates [37,38]. Burgess and Summers [39] and Summers [40] have discussed the effect of the radiation field, and of collisions, on the dielectronic recombination rate, which can be reduced by the re-ionization (by optical photons or low energy electrons) of the recombined, but still highly excited, ion. Radiation effects are relatively unimportant in the solar corona, except in the case of the relative population of metastable fine structure levels such as the ^3P and ^3S levels in helium-like ions [3] and the 2s2p ^3P levels in beryllium-like ions [26], which can be influenced by the radiation field of the photosphere. However, for strong non-solar sources, it cannot be assumed that the high energy photon field is dilute, and photoionization processes may completely dominate the ionization equilibrium. Tarter, Tucker and Salpeter [42], and Tarter and Salpeter [43] have discussed the

ionization equilubrium which results if the spectrum of the radiation field is in the shape of thermal bremsstrahlung. For a wide range of conditions, the ionization equilibrium and the electron temperature depend only on two parameters, the bremsstrahlung temperature, T_x, and the normalized radiation flux,

$$\xi(r) \equiv L/Nr^2 \qquad (3)$$

where L is the source luminosity, N the ion density, and r the distance from the radiation source (spherical symmetry has been assumed). Ionization equilibrium curves have been computed for optically thin [42] and optically thick [43] environments. For objects in which the density is too low for LTE to be established, but for which the x-ray radiation field cannot be considered dilute, techniques for the direct determination of the ionization equilibrium will be of considerable importance. The extended accretion zones of x-ray binary sources, and possibly the interstellar shocks of young supernovae remnants, should fall into this class of object.

III. THE X-RAY OPACITY OF THE INTERSTELLAR MEDIUM

The interstellar medium is important to cosmic x-ray astronomy for two reasons:

1. The x-ray opacity of the ISM determines the distance at which a source can be observed in a given wavelength.
2. X-ray observations of the wavelength structure of the x-ray opacity of the ISM offer a number of unique capabilities for the study of the abundances and ionization structure of the ISM, and of the composition and size of the interstellar grains.

The prospects for soft x-ray astronomy have been reviewed recently by Cruddace et al. [44]. It has now become clear that the interstellar medium is highly inhomogeneous, consisting of dense H I clouds at low temperature, which are contained by a hot, weakly ionized intercloud medium. The volume occupied by the H I clouds is small, and consequently, the high transparency of the intercloud medium will allow the observation of XUV sources over a considerably greater distance than had been previously thought. Earlier pessimistic prospects for soft x-ray astronomy were based on the work of Strom and Strom [45] whose calculation for a particular direction with high interstellar density ($N_H > 1$ cm^{-3}) has been taken by many authors as typical. The review by Pikelner [46] shows that the intercloud medium has a density of $N_H \sim 0.1$ cm^{-3} or less in many directions. The earth is in fact embedded in a region of low density. Confirmation of the low density of the interstellar medium in the vicinity of the earth has been provided by the work of Seward et al. [47] who have analyzed observations of x-ray sources over a broad wavelength range to determine the column density of hydrogen to each source. In particular, they have used the observation of supernovae

remnants whose distances are known to determine the column density per cubic centimeter for sources near the earth. They find that, while for sources near the galactic center mean column densities exceed $N_H \sim 1$ cm^{-3}, for sources closer than 1 kiloparsec the mean density is less than $N_H \sim 0.2$ cm^{-3}. For sources even closer, or for a selected direction, the evidence that N_H is less than or about equal to 0.1 cm^{-3} is now extremely strong. Details of these "local" observations of the ISM will be presented later in this section. In Figure 3, the distance at which the optical depth of the ISM is 2.3 (attenuation of the incident flux by a factor of 10) for wavelengths between 1 and 1000Å is shown for densities ranging from 0.03 to 0.2 cm^{-3} [44]. Observations of the star γ^2 Vel, which is 460 pc-distant [48] by the European Orbiting Spectrophotometer, S59, have indicated the mean density of neutral hydrogen is 0.02 cm^{-3} in this direction, indicating that observations of objects at 100Å out to 500 pc in certain directions may be possible. We can certainly expect to see local sources at wavelengths beyond 300Å, and we should expect that normal to the galactic plane, extragalactic objects should be visible out to $\sim$ 100Å.

In this section I discuss techniques which have been proposed for the study of the structure of the ISM with x-ray observations, and current models of the x-ray opacity of the ISM.

III.A TECHNIQUES FOR THE STUDY OF THE INTERSTELLAR MEDIUM

The interaction of x-rays with the interstellar gas is dominated by absorption, and may be described by the optical depth for absorption, τ_a

$$\tau_a(\lambda) = n_H \left\{ a_{H_2} \sigma_{H_2} + \sum_Z a_{Zz} A_Z \sigma_{Zz}(\lambda) \right\}$$

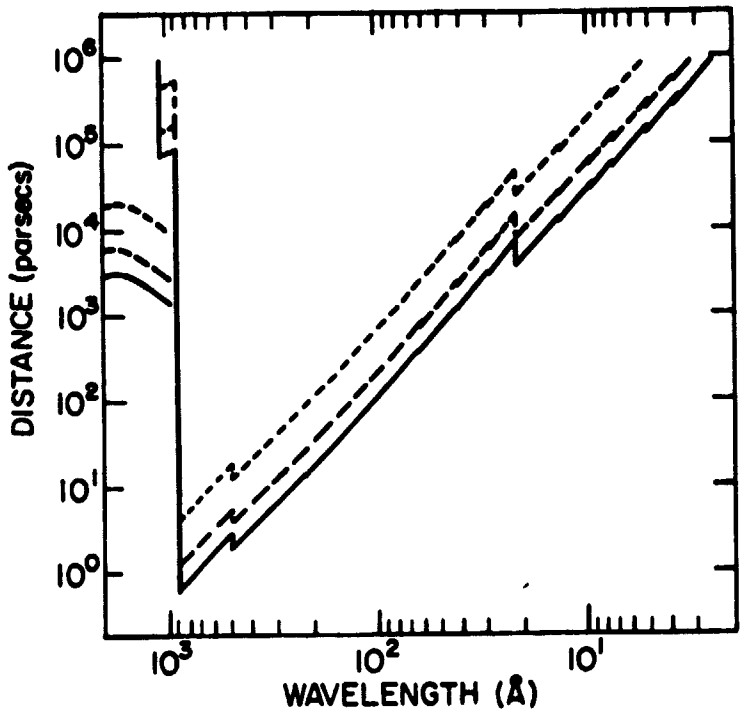

Fig. 3. Distance at which attenuation of the incident radiation reaches 90 percent, as a function of wavelength. An un-ionized interstellar medium of normal composition is assumed, and the contribution of the dust above 100Å is included. —— n_H = 0.2 cm^{-3}; — — n_H = 0.1 cm^{-3}; ---- n_H = 0.03 cm^{-3}. (After Cruddace et al., Ref. 44)

where n_H is the total hydrogen column density in all states (molecular, atomic, and ionized), a_{H_2} is fraction of hydrogen which is molecular, a_{Zz} is the fraction of ions of element Z (abundance A_Z) which are in ionization stage z, and σ_{Zz} is the absorption cross-section. The fractional population of all molecules except H_2 is sufficiently small that they may be neglected. Early studies of the x-ray opacity of the ISM [45,49,50,51] assumed that the medium is entirely gaseous and neutral. Quite obviously, the relative strength of the absorption edges observed in the spectra of individual sources can be used to determine the relative abundance of elements in the intervening ISM between earth and source [52]. The inclusion of the effects of the ionization structure of the gas and the effects of the interstellar grains result in modifications to the spectral shape of the x-ray opacity of the ISM which will, in turn result in observable effects in the spectra of strong sources. The observation of these effects should allow unique tests of a number of models of the characteristics of the ISM.

The effects of ionization are two-fold;

1. The absoprtion edge of ions in the ISM will be shifted in wavelength from the edge of the neutral atom.
2. The absorption cross-section of singly ionized helium is approximately half that of neutral helium, and the absorption cross-section of ionized hydrogen is zero.

The presence of grains in the interstellar medium modifies the x-ray opacity in four ways.

1. The grains have an appreciable scattering cross-section as well as absorption cross-section. The radiation is scattered primarily at very small angles and forms a halo of radiation around a point source.
2. The scattering which causes the halo becomes anomalous at wavelengths near an absorption edge.

3. Saturation effects occur in x-ray absorption if the thickness of an individual grain significantly exceeds unit optical depth.

4. The K absorption edge of material in a grain is more complex than the absorption edge of a gas. In addition, to chemical shifts of the edge wavelength, there is an oscillatory behavior of the cross-section on the high energy side of the absorption edge [53].

Overbeck [54] gives the approximate relation

$$\alpha_{1/2} \sim 10\ \lambda/a \quad ,$$

for the fwhm angle of the scattering halo, where λ is in angstroms, and a, the grain diameter, is in microns. The size of the halo will be typically 1' to 1° in the wavelength range 1 - 30Å.

Martin [53] and Hayakawa [55] have calculated the size of the scattering halo around a point x-ray source, for various assumptions about the size distribution of the interstellar grains. If the absorption optical depth of the gas and grains are τ_a and τ_{ag} respectively, and if τ_{sg} is the scattering optical depth for the grains, the intensity in the core is $\exp[-(\tau_a + \tau_{ag} + \tau_{sg})]$, and the total intensity in the scattering halo is $\exp[-(\tau_a + \tau_{ag})]\{1 - \exp[-\tau_{sg}]\}$. For a source distance of 1 kiloparsec, Martin predicts that the intensity in the halo will be ~ 10% of that in the core.

The anomalous scattering near an absorption edge can obviously be useful in studying the composition of the grains. Martin, and Martin and Sciama [56] discuss this point in detail. The scattering cross-section becomes smaller, by as much as a factor of ~8, so that

the energy in the halo will be much smaller near the absorption edge. If we are able to image the halo in narrow wavelength bands, such an effect may be observable for those elements which are major constituents of the grains.

If the individual grains are sufficiently thick, self-blanketing will occur, and the effective cross-section of the elements bound in grains will be reduced. Fireman [57] has computed the magnitude of this effect for a number of grain models. Reduction of the opacity by factors between 10 and 30% can occur for realistic grain models.

Recently Cruddace et al. [44], Fireman [57] and Ride and Walker [58] have developed more sophisticated models of the opacity of the ISM which include many of the interaction mechanisms which have been discussed in the foregoing paragraphs. The model of Cruddace et al. includes the effects of ionization structure, and the model of Fireman includes the effects of self-blanketing in the grains. Ride and Walker have developed a model of the x-ray opacity in the direction of the Crab nebula which includes the effects of ionization structure, self-blanketing in the grains, and chemical evolution in the galaxy. In the following section this model is examined in more detail to illustrate the effect of the interaction mechanisms which have been discussed.

III.B MODELS OF THE STRUCTURE OF THE INTERSTELLAR MEDIUM

The Crab nebula is an ideal candidate for analysis of the structure of the ISM, it is a strong x-ray source, and the intrinsic spectrum is well determined. The Crab is also a strong radio source, and extensive data is available on the column density of neutral hydrogen, and of a number of molecules which are associated with clouds. There is now

ample evidence that the ISM exists in two phases; with cool high density ($n_H \sim 10 - 10^3$ cm^{-3}) clouds embedded in a hot low density ($n_H \sim 0.03 - 0.1$ cm^{-3}) intercloud medium (ICM) [59]. Most elements are singly ionized in the ICM, and a substantial fraction of most elements appear to be bound in the grains [60,61]. Morton [62] has summarized the Copernicus observations of interstellar abundances in the direction of the unreddened star ζ Oph. Morton's results are summarized in Figure 4. The deficiency of most abundances with respect to solar abundances observed by Morton presumably reflects the depletion of atoms in the gas by the grains.

Ride and Walker [58] have carried out a detailed study of the structure of the ISM in the direction of the Crab nebula. They used a two component model of the ISM, consisting of clouds, and an intercloud medium, and including the effects of grains and the ionization structure, and the effect of the chemical evolution of the galaxy on abundances. The parameters chosen for the ISM model are summarized in Table III, where a_{Zz} is the fractional abundance of ionization stage z of element Z, and β_Z is the fractional depletion of element Z onto grains. Radio observations of the Crab indicate that half of the material in the line of sight is in clouds, and half in the intercloud medium. Previous analyses of the x-ray opacity of the ISM in the direction of the Crab nebula found that the observed radio column density was inconsistent with the observed x-ray attenuation of the Crab spectrum, unless anomalous enhancements of the abundance of certain elements with respect to solar abundances was assumed. Ride and Walker used a model of the chemical evolution of the galaxy developed by Talbot and Arnett [63] which predicts a 20% enhancement of all metal abundances (by metals we mean all elements heavier than helium) in the ISM, with the exception of nitrogen

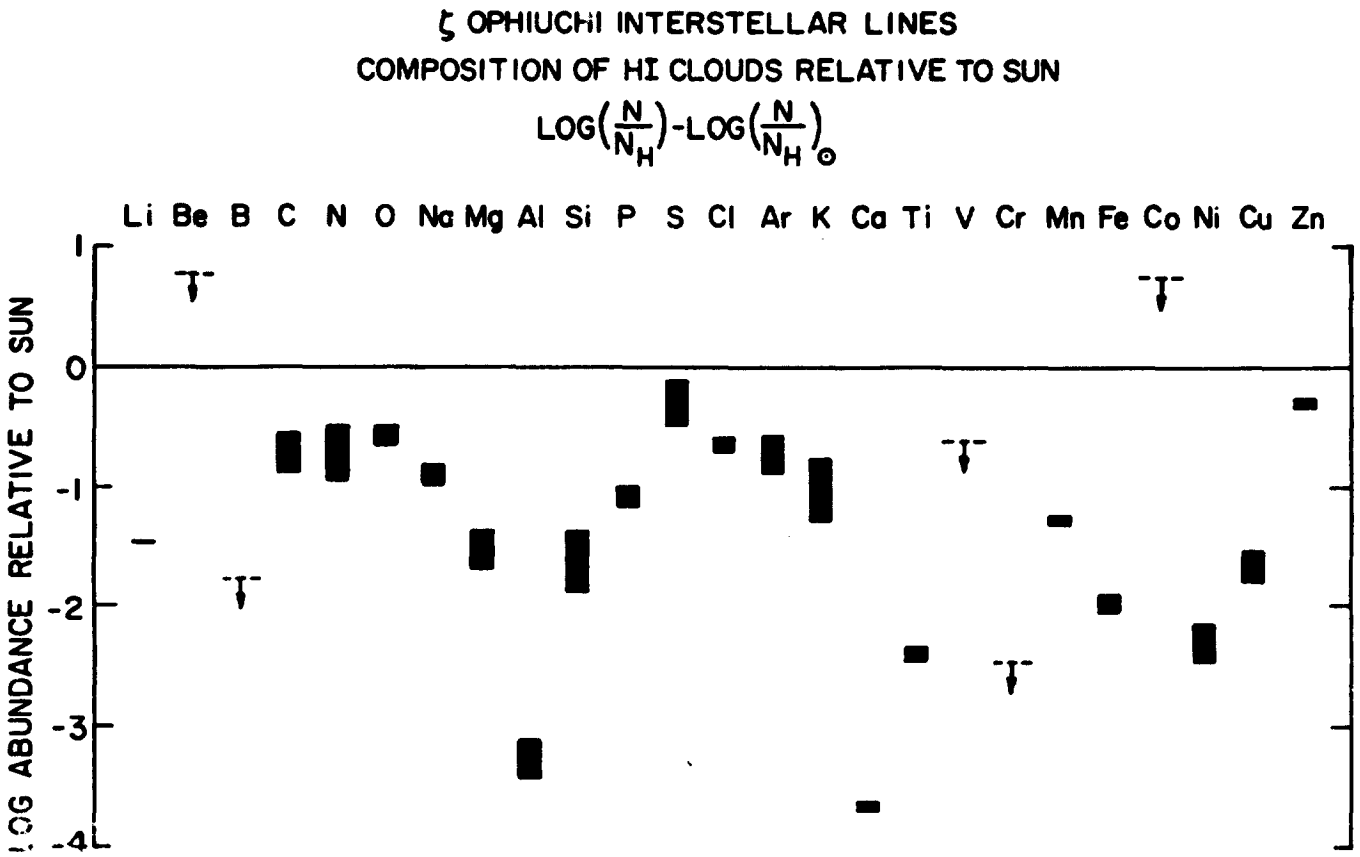

Fig. 4. Composition of H I clouds in the direction of ζ Oph, relative to the sun. An element lying below the horizontal line is depleted compared with its solar system abundance. Ions such as N II and Si III, which are expected to be entirely in H II regions, were not included. The lengths of the vertical bars mainly indicate the uncertainties in the curve of growth, though in some cases the bars were lengthened when errors in equivalent widths or f-values were important. (After Morton, Ref. 62)

TABLE III

IONIZATION STRUCTURE OF THE INTERCLOUD MEDIUM
(UV Ionization)

	H	He	C	N	O	Ne	Mg	Si	S	Ar	Fe
$a^{ICM}_{Z\,I}$	0.83	1.0	0	0.8	0.85	1.0	0	0	0	0	0
$a^{ICM}_{Z\,II}$	0.17	0.0	1.0	0.2	0.15	0	1.0	1.0	1.0	1.0	1.0

IONIZATION STRUCTURE OF THE CLOUDS

	H	He	C†	N	O	Ne	Mg†	Si†	S	Ar	Fe†
$a^{c}_{Z\,I}$	0.85*	1	0	1	1	1	0	0	0	0	0
$a^{c}_{Z\,II}$	0	0	1	0	0	0	1	1	1	1	1

FRACTIONAL DEPLETION OF ELEMENTS ONTO GRAINS

	H	He	C	N	O	Ne	Mg	Si	S	Ar	Fe
β^{ICM}_{Z}	0	0	0.8	0.5	0.5	0	0.8	0.5	0.3	0.5	0.8
β^{c}_{Z}	0	0	1	0.9	0.9	0.1	1.0	1.0	0.7	0.9	1.0

*15% of the hydrogen is assumed to be in the form of molecular hydrogen.

†The ionization structure of these elements in clouds is given for the sake of completeness. However, Ride and Walker ignore the small fraction of these elements in clouds which are not bound in grains.

which was assumed to be enhanced by 40%. The relative abundances used are given in Table IV. Ride and Walker computed the opacity of the ISM for three models, an entirely gaseous and neutral ISM (Model I), an ISM with the parameters given by Table III and with 0.3 micron grains (Model III), and an identical model, with the exception of an increased grain size of 1.2 microns (Model II). The parameters of the models are summarized in Table V, and the calculated opacity for each model is shown in Figure 5. Model III predicts a neutral hydrogen column density of 2.15×10^{21} cm^{-2}, in good agreement with the radio value of 1.8×10^{21} cm^{-2}. Model I, in contrast predicts $n_H \sim 3.0 \times 10^{21}$ cm^{-2}. On the basis of low resolution x-ray observations alone, it is not possible to reject models which have anomalous abundances for 1 or 2 elements, such as the model fitted to their observations by Charles et al. [64], which assumes that neon is enhanced by a factor of 7 in the ISM, compared to the (somewhat uncertain) solar neon abundance. However, we can construct realistic ISM models which fit the x-ray and radio observations, and which do not require drastic assumptions concerning ISM abundances. Figure 6 compare the magnitude of the strongest absorption edges for three strong sources [65]. The equivalent neutral hydrogen column densities to a number of strong sources have recently been discussed by Gorenstein [66] and by Ryter, Cesarsky and Audouze [67]. The use of more recent observations results in a number of differences from the compulation of Seward et al. [47].

III.C THE INTERSTELLAR MEDIUM IN THE VICINITY OF THE EARTH

In the preceding sections we discussed the opacity of the ISM primarily as a tool for the study of the structure and composition of the ISM. The "local" opacity of the ISM is decisive in determining

TABLE IV

ADOPTED ISM ABUNDANCES

H	10^6	Mg	40
He	7×10^4	Si	39
C	444	S	19
N	165	Ar	4.5
O	811	Fe	31
Ne	130		

TABLE V

MODEL PARAMETERS FOR THE ISM

Quantity	Model I	Model II	Model III
$\alpha^{\dagger}$	0	0.5	0.5
$a^{c}_{H_2}$	0	0.15	0.15
d^{*}	--	1.2μ	0.3μ

*Grain size in microns.

†Fraction of material in the ISM in clouds.

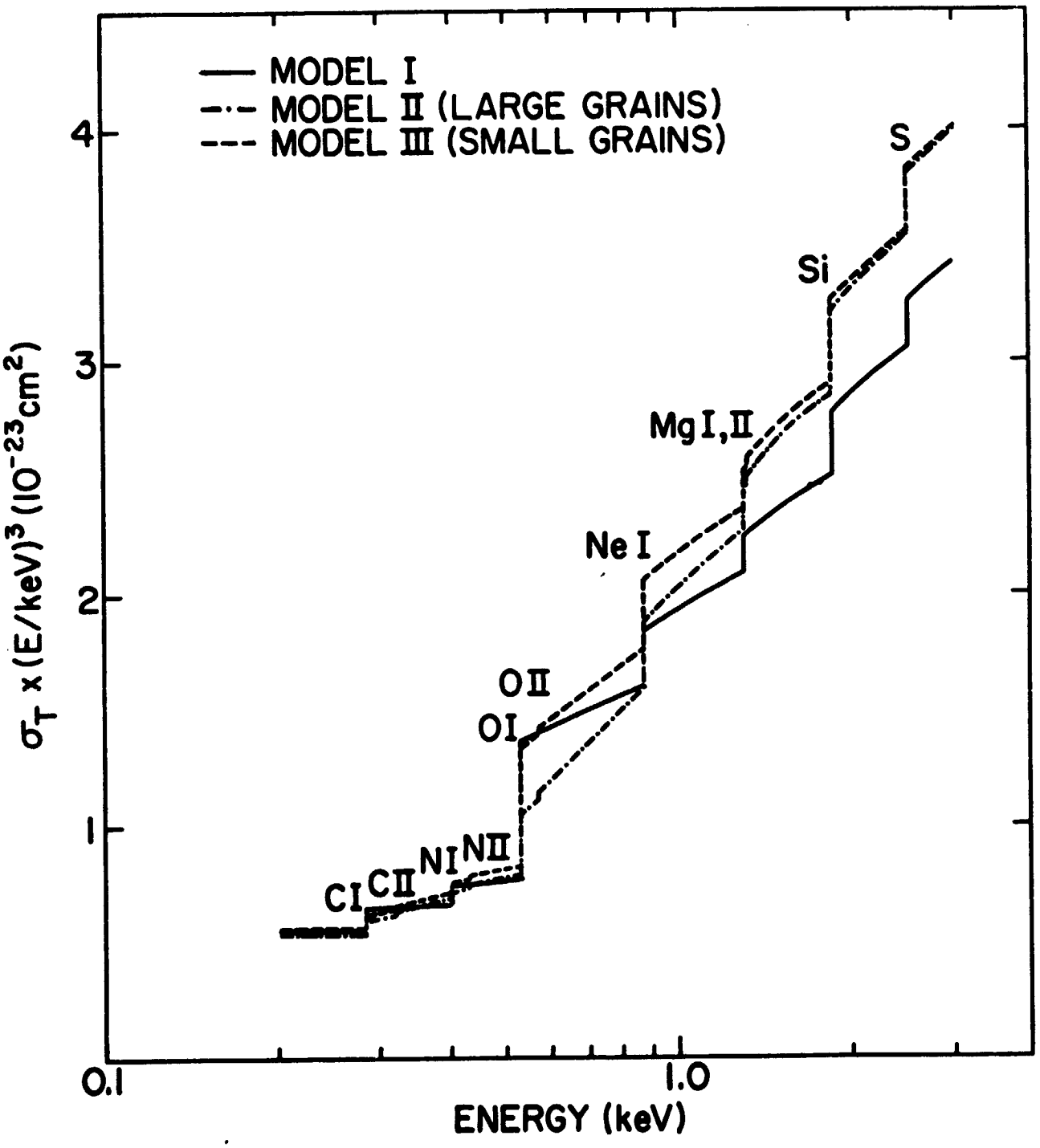

Figure 5. X-ray opacity of the ISM for three models. (After Ride and Walker, Ref. 64)

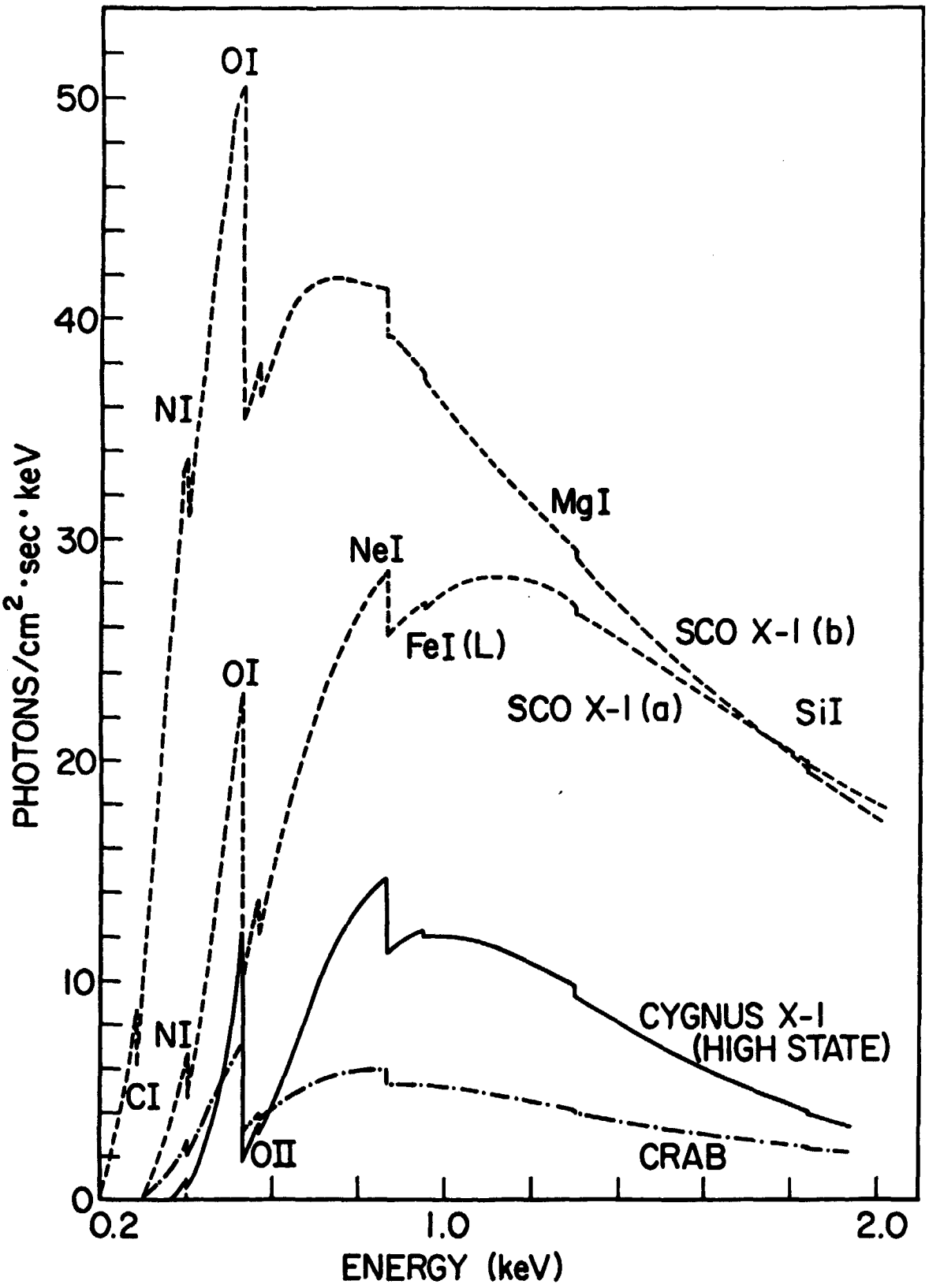

Fig. 6. Computed spectra for three strong x-ray sources. Solar abundances have been used in this computation, and calculations have been carried out for two assumed values of the column density in the direction of Sco X-1, which appears to be somewhat uncertain at present. The values of the hydrogen column density used are: Sco X-1 curve (a) - 1.5×10^{21}, curve (b) - 2.0×10^{21}; Cygnus X-1 - 7×10^{21}; and the Crab - 2.6×10^{21}. (After Ride, Ref. 65)

our ability to observe soft sources. A number of observations of interstellar absorption lines in the spectra of nearby stars have recently been carried out. Recent determinations of the local ISM density are summarized in Table VI. The value of $N_H \sim 0.1$ cm^{-3} appears to be an upper limit to the local ISM density, and the mean density in many directions appears to be significantly lower. Evidence strongly supports a very local (< 1-5 pc) density which may be as low as 0.01-0.03 cm^{-3}. Reviews of determinations of ISM density out to $\sim$ 100-200 pc have been presented by a number of authors [68].

The results on the local density of the ISM presented in Table VI have important implications for spectroscopic studies of cosmic x-ray sources. For example, at 600Å, for a mean ISM density of $N_H = 0.03$ cm^{-3} 10% of the incident flux is transmitted at 10 pc, and at 20 pc 10% of the flux is transmitted out to 400Å. For objects within 5 pc, all wavelengths are attenuated less than 90%. According to Van der Kamp [69] there are 60 stars within 5.2 pc, of which 54 are main sequence stars, including three of near solar type. There are approximately 1000 stars within 20 pc [69]. If a sizable fraction of these objects emit radiation as efficiently as the sun at wavelengths below $\sim$ 500 - 600Å, a substantial number of soft x-ray objects should be observable with suitable instrumentation.

TABLE VI

DETERMINATIONS OF THE "LOCAL" DENSITY OF THE INTERSTELLAR MEDIUM

Star	Distance pc	Spectra	Column Density N_H/cm^{-2}	Mean Density N_H/cm^{-3}	Local Density N_H/cm^{-3}	Reference
α C.Mi (Procyon)	3.5	F5 IV	1.6×10^{17}	--	0.015	Evans et al. [133,138]
β Gem (Pollux)	10	K0 III	$3\text{-}12 \times 10^{17}$	--	0.03 - 0.15	McClintock et al. [135]
α Boo (Arcturus)	11.1	K2 III	$3\text{-}12 \times 10^{17}$	0.02 - 0.10	--	Moos et al. [139]
α Aur (Capella)	14	G5 III/G0 III	4×10^{17}	0.01	--	Dupree [137]
α Tau (Aldeberan)	20.8	K5 III	$1.2\text{-}3 \times 10^{18}$	< 0.2	--	McClintock et al. [135]
α Leo (Regulus)	22	B7 V	1.3×10^{18}	0.02	--	Rogerson et al. [140]
α Eri Achernan)	28	B3 IV	6×10^{18}	0.07	--	Rogerson et al. [140]
λ Sco	112	B1.5 IV	2×10^{19}	0.072	--	York [140]
ν Sco	151	B2 IV	2.2×10^{19}	0.05	--	Rogerson et al. [140]
γ^2 Vel	460	--	2.7×10^{19}	0.02	~ 0.1	Grewing et al. [48]

IV. THE NATURE AND SPECTRA OF INDIVIDUAL COSMIC X-RAY SOURCES

A general review of the characteristics of individual cosmic x-ray sources is contained in the recent book edited by Giacconi and Gursky [70], and in the recent reviews by Culhane [71]. The present discussion concentrates on the spectral characteristics of the most important classes of sources, and on the observations and analytical techniques which should prove useful in the study of the structure and composition of these objects. The strongest, and most frequently observed objects fall into two classes; the remnants of supernovae explosions which are intense extended sources of x-rays, and compact objects in which the x-rays are generated by accretion of matter onto a highly evolved star in a binary system. Williamson et al. [72] have recently identified a new class of x-ray object, extended regions of soft emission in our galaxy. These regions of enhnaced diffuse emission may be the manifestation of very old supernovae remnants [73,74], or of a galactic halo. Interpretation of the structure of the low energy background [75] has suggested the existence of a class of soft x-ray source with high space density ($\approx 10^{-2}$ pc^{-2}) and moderate ($\approx 10^{31}$ - 10^{34} ergs/sec) luminosity. It is possible that the extended regions of soft emission found by Williamson et al. may explain the observed excess in the soft x-ray background, without additional discrete sources. For these three classes of observed x-ray objects reasonably detailed models of spectral structure may be developed.

Some authors [75,76,77] have suggested that the observed soft x-ray background may be identified with the coronae of normal main sequence or giant stars. Recent ultraviolet observations with the Copernicus

satellite have provided strong evidence for coronae in several nearby stars, and recent observations have identified two nearby stars as soft x-ray sources. By analogy with the coronal spectrum, it appears probable that the spectra of stellar coronae will resemble the line rich spectrum of the solar corona.

One class of extragalactic source, the x-ray emission from the intercluster gas in rich Abell clusters of galaxies, is sufficiently well studied to allow spectral models to be developed.

IV.A SUPERNOVAE REMNANTS

The general characteristics of supernovae remnants (SNRs) have been reviewed by Wolter [78] and by Shklovsky [79]. A substantial fraction of the energy released by a supernovae explosion is stored in the rotational energy of a rotating magnetized neutron star (pulsar), and in the expansion of the outer stellar layers which are ejected in the explosion. The release mechanisms of both modes of stored energy result in the emission of x-rays; in the case of the pulsar by energetic processes at the magnetic poles, and by the release of high energy electrons which radiate by synchrotron emission in the weak magnetic field associated with the optical nebula observed with young SNRs, and in the case of the ejecta by the formation of an interstellar shock wave as the ejected material interacts with the ambient ISM. The non-thermal pulsar spectrum and the synchrotron emission are not likely to contain strong spectral features, although the intrinsic regularity of these spectra make young supernovae remnants, which radiate primarily by these mechanisms, useful as probes of the ISM. As the central pulsar slows, the spectrum is dominated by radiation from the interstellar shock wave created by the ejecta. It is the spectrum generated by the interstellar shock which is the major focus of the present discussion.

IV.A.1 MODELS OF SUPERNOVAE REMNANTS

A number of authors have developed models of the interstellar shock developed by a SNR [80-87]. The work of Cox [81] is representative of the analytical models, which describe a spherically symmetric shock using relatively few parameters; W_0, the total energy released; M_e, the ejected mass; M_{sw}, the mass of the material swept up by the ejecta; V_s, the velocity of the shock; t, the age of the SNR; N_1, the density of the ambient ISM prior to the supernovae explosion; and r, T_i, and T_e, the radius, ion and electron temperature of the shell-like shock which is responsible for the majority of the x-ray emission. The analytical models predict three phases in the evolution of a SNR, an early phase during which $M_e \gg M_{sw}$, the adiabatic phase during which $M_{sw} \gg M_e$, but radiative losses have not yet become important, and a radiative phase during which the remnant shell cools. During the early phase the shock forms a thin shell with $\Delta R \sim R/12$. The predicted temperatures are between 10^7 and 10^9 ^oK, the shell is optically thin and the emission should be strongest between 1 and 100 keV. During this phase, the ion temperature may significantly exceed the electron temperature. During the adiabadic phase, the predicted temperature is in the range from ($1 - 10 \times 10^6$ ^oK) and the shell radius is in the range $\sim 10 - 20$ pc. During the radiative phase the shell temperature falls below 10^5 ^oK, and the x-ray emission will be dominated by the hot low density gas interior to the shockwave shell.

More sophisticated numerical models of the SNR generated interstellar shock [84,86,87] predict the development of a second, inward propagating shock which is caused by the deceleration of the ejecta by the ambient

ISM. The higher density behind the shock may result in the x-ray emission from this reverse shock becoming dominant in the spectrum of young SNRs. These more sophisticated models, although still assuming spherical symmetry and a uniform ambient ISM, predict density inhomogeneities such as the observed fast optical filaments [87] and a non-isothermal configuration for the remnant. The density and temperature distributions predicted for a remnant with initial parameters $M_e = 0.64\ M_\odot$, $W_0 = 3.2 \times 10^{50}$ ergs, and thermal energy $E_T = W_0/47.2$ expanding into an ISM with $N_1 = 1\ cm^{-3}$ and $T_0 = 2 \times 10^4\ ^oK$, by the calculations of Mansfield and Salpeter [84] are shown in Figures 7 and 8 for ages 10^3, 3×10^4 and 5×10^4 years. The dependence of emission measure on the square of density will result in the dominance of the radiation from material near the shock front in the overall spectrum of the remnant. Many of the features of the detailed computational models are contained in the analytical models, however there are differences which should have observable effects on the spectrum. An example is the existence of material inside the shell at temperatures greater than the shell temperature, which will result in a harder x-ray spectrum for a given shock velocity.

IV.A.2 OBSERVATIONS OF THE X-RAY SPECTRUM AND STRUCTURE OF SUPERNOVAE REMNANTS

Ilovaisky and Ryter [88] and Gorenstein and Tucker [83] have reviewed observations of the x-ray spectra of SNRs. Seven remnants have been definitely observed in x-rays (the Crab nebula, Cas A, Tycho, Pup A, Cyg Loop, Vela X and Lupus), and six others probably observed. The spectrum of the Crab nebula appears to be dominated by the pulsar, and by synchrotron radiation from relativistic electrons. Of the five

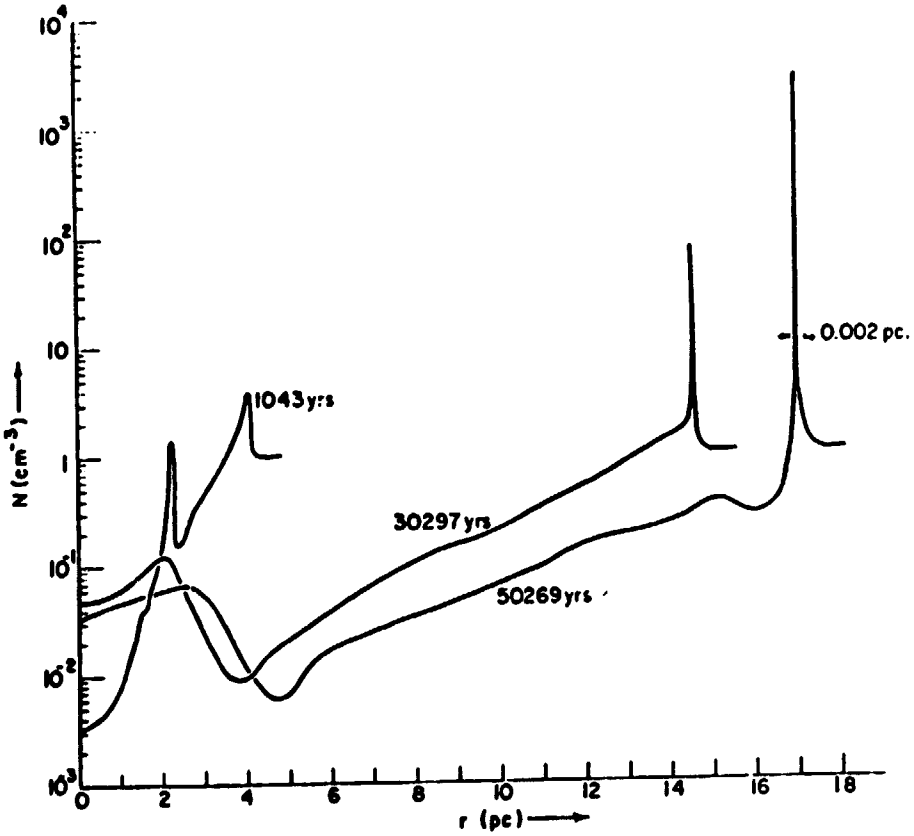

Fig. 7. The number density as a function of distance. The time in years labels each curve and the thickness of the shell for which $N > 10$ cm^{-3} is shown on the last curve. (After Mansfield and Salpeter, Ref. 84)

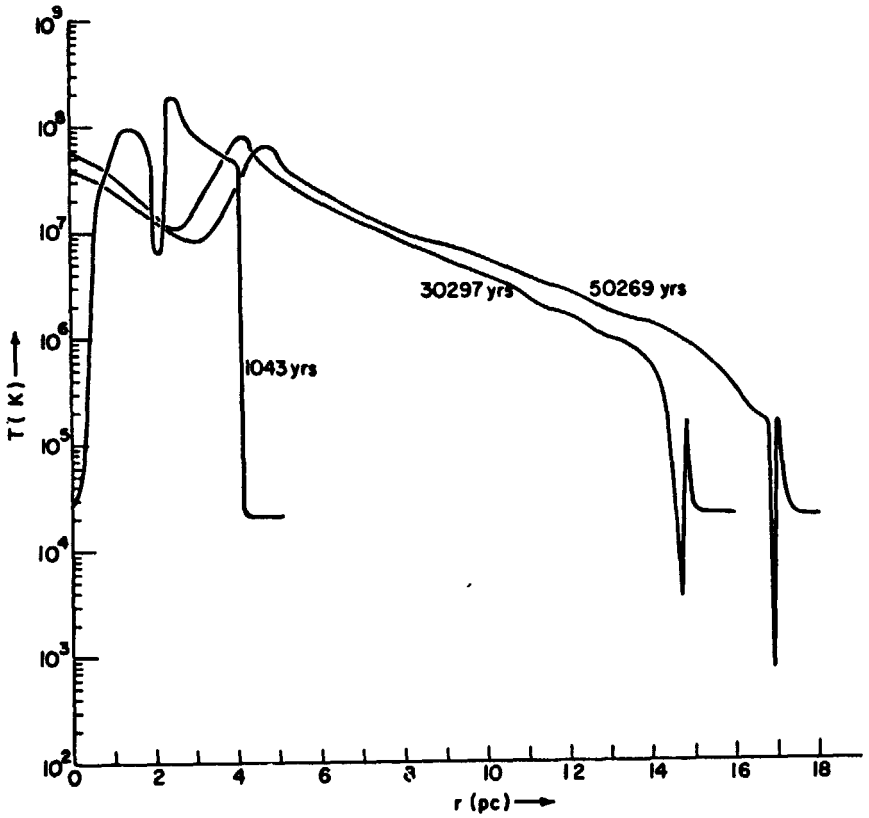

Figure 8. The temperature as a function of distance. The time is years labels each curve. (After Mansfield and Salpeter, Ref. 84)

remaining intense objects, two (Cas A and Tycho) appear to be in the early phase, and the remaining three (Pup A, Cyg Loop and Vela X) in the adiabadic phase. Gorenstein et al. [82] have used the available observations to derive parameters for isothermal shock wave models. These parameters are given in Table VII. The model parameters are in reasonable agreement with the observed properties for the three older remnants. For the younger remnants, Cas A and Tycho, the spectra are more complex than predicted by the analytical shock wave model, and the effects of the "reverse shock wave" [86] must be included to obtain reasonable values for N_1. The isothermal spectral fits obtained by Gorenstein et al. and by others [83] to the spectra of Pup A, the Cygnus Loop and Vela X are superior to the fits obtained for power law spectra or other shapes.

The SNR models discussed above have assumed a spherically symmetric ISM. Inhomogeneities in the ambient ISM will result in structure in the x-ray emitting shell-like interstellar shock. Studies of the spatial structure of SNRs [89,90,91 and the references contained therein] have indeed found such structure.

IV.A.3 ANALYTICAL TECHNIQUES FOR THE STUDY OF SUPERNOVAE REMNANTS

The optically thin nature of the spectra of SNRs makes all of the spectroscopic techniques discussed in Section II applicable to the spectra of these objects. As discussed above, the development of thermal models with low resolution observations is difficult because of questions on relative abundances [92], and on the nature of the ionization equilibrium. These problems are most pronounced for young SNRs. The diagnostic techniques for the study of relative abundances and the ionization equilibrium will be of major importance for these objects.

TABLE VII

SUPERNOVA SHOCK WAVE MODEL PARAMETERS

Object	T(^{o} K)	2R(pc)	N_1 (cm^{-3})	$M_{sw}/M_{\odot}$	W_0 (ergs)	t (years)	V_s(km s^{-1})	T_1(^{o}K)*
Cas A	1.5×10^7	4.5	7 1†	8 6†	3×10^{51} 2×10^{51}†	150-400††	6,000	4×10^8
Tycho	1.0×10^7	6	5 2†	14 10†	2×10^{51}	400	3,000	1×10^8
Pup A	7×10^6	17	0.6	40	3×10^{50}	4,000	800	7×10^6
Cyg Loop	3×10^6	38	0.15	100	4×10^{50}	17,000	500	3×10^6
Vela X	4×10^6	40	0.08	60	4×10^{50}	13,000	600	4×10^6

NOTE -- M_{sw} = swept-up mass

*Ion temperature

†Reverse shock wave model (McKee, Ref. 86)

††Age depends on assumed evolutionary phase

(After Gorenstein et al., Ref. 83)

Once these parameters are approximately established, an analysis based on equation (1) should result in a complete thermal model, and a refined set of relative abundances. The low surface brightness of even the most intense SNR sources will make observation of lines difficult. Consequently, the observing program must be carefully planned in advance, and the use of grating spectrographs, which can record a substantial number of lines simultaneously, is to be preferred whenever possible.

IV.B COMPACT X-RAY SOURCES

A number of the intense compact x-ray sources within our galaxy, and in the neighboring Magellanic Clouds, have been identified with binary systems. For many of the compact objects which have not been definitely identified with binary stars, such as Sco X-1, the evidence that they are representatives of the same calss is now quite strong. Tannenbaum and Tucker [93] and Blumenthal and Tucker [94] have recently reviewed the propcrties of this class of object, and a number of the most interesting individual objects, in depth. In the present discussion, emphasis will be placed on the spectral features which may be expected in spectra of this class of object. The basic spectrum is generated near the collapsed object, neutron star, white dwarf, or black hole, by the release of gravitational energy in the process of accreting matter from a "normal" companion. The spectrum will be significantly modified by the atmosphere of the collapsed object, and will in turn create an ionization zone, analogous to the Strömgren sphere created around an ultraviolet star.

IV.B.1 SPECTRAL MODELS FOR ACCRETION SOURCES

The general properties of the accretion disk surrounding the collapsed object in a binary source, and of the resultant x-ray spectrum have been discussed by a number of authors [95-104]. The general spectral shape observed with low resolution detectors for these objects may be approximately fit by thermal bremsstrahlung curves [47], although many objects display a harder spectral component in addition. The theoretical models suggest that the accretion disks are not isothermal, and are optically thick [97,98], consequently, high resolution spectroscopy is likely to reveal a more complex spectral shape for the continuum spectrum of these sources, which may approach a Wein spectrum. We are concerned here with spectral structure in these objects, which can result from four effects:

1. The production of emission lines in the intrinsic spectrum generated within the accretion disk.
2. The generation of lines by fluorescence and heating in the atmosphere of the companion star.
3. Absorption of the soft component of the intrinsic spectrum by the outer portions of the accreting material (stellar wind). Variable cutoff energies are expected for some objects.
4. The emission spectrum of the photoionized outer regions of the accreting material.

Felten and Rees [105] and Felten, Rees and Adams [106] have discussed the radiative transport of x-ray line photons in x-ray binary sources with homogeneous isothermal atmospheres, and have carried out specific calculations for Sco X-1. The principal sources of opacity are free-free scattering and Thomson scattering, however resonance scattering for allowed lines can substantially increase the effective path length of line photons before emerging from an optically thick atmosphere. For

most binary sources, the accretion disk temperature is sufficiently high ($T > 5 \times 10^7$ °K) that the principal emission mechanism is thermal bremsstrahlung, so that the intrinsic spectrum consists of a continuum with relatively weak line emission, due principally to radiative recombination, except in the case of iron lines where direct collisional excitation remains important. The opacity introduced by the optically thick nature of the source results in the broadening of these lines so that the observational line profile will consist of a weak core, broadened by the thermal Doppler effect, and a broad Thomson scattered main line. Felten, Rees and Adams [105] have calculated the shape of the line profiles for a model Sco X-1 atmosphere with a temperature of 5×10^7 °K, and with an optical depth of 10. Some of their results are summarized in Table VIII. Attempts to observe these weak line cores in Sco X-1 have, so far, proved unsuccessful. (Observational results are discussed in Section IV.B.3.)

Mészáros [120] has discussed the line shapes to be expected for accretion disk models, specifically for the case in which the accreting object is a black hole. Depending on the parameters of the model chosen (mass of black hole, accretion rate and efficiency of transport of angular momentum) equivalent widths for the $2\,^2S - 1\,^1S$ and $2\,^3P - 1\,^1S$ line cores in Fe XXV are ≤ 1 eV. The shape of the line core will, however, be different from that expected for a static atmosphere, since thermal Doppler broadening will be dominated by rotational and gravitational broadening. Rotational broadening will depend on the orientation of the spin axis of the accr ting black hole, but will generally exceed 200 eV, and gravitational broadening may be as large as 30-60 eV. Consequently, line widths in the core will certainly exceed 100-200 eV.

TABLE VIII

SPECTRAL LINE PROFILES IN Sco XI

	Doppler Width	Thomson Width	I(core)/I(total)	Equivalent Width of Line Core
S XVI Lyα	0.2%	16%	0.016	0.18 eV
O VIII Lyα	0.15%	12%	--	$\sim$ 10 eV
Fe XXVI Lyα	0.2%	16%	0.005	1.9 eV
Fe XXV $^1S - {}^3P +$ $^1S - {}^3S$	0.2%	16%	0.25	13 eV
Fe XXV $^1S - {}^1P$	0.2%	16%	0.05	0.57 eV

Note: The results quoted are for 5×10^7 ^oK and an optical depth of 10.

(After Felten, Rees and Adams, Ref. 106)

Basko, Sunyaev and Titarchuk [108] and Milgrom and Salpeter [109] have discussed radiation processes which occur near the surface of the normal star in a binary system as a result of the illumination by the intense x-ray flux from the compact object.

Two processes occur, a substantial fraction ($\lesssim \sim 30\%$) of the incident flux may be re-emitted at x-ray wavelengths, while the remaining energy is re-emitted at longer wavelengths. This effect may be especially important for binaries which contain x-ray pulsars, since the reflected beam will be the only x-ray flux observed if the earth is not in the path of the pulsed beam. The fraction of directly scattered photons increases with energy, and this effect becomes dominant at energies $h\nu \sim 8$ keV. The spectrum of the reflected x-ray should contain structure due to increased photoabsorption at the edges of the abundant heavy elements, especially Fe, where the jump in reflected energy flux across the edge may exceed a factor of 2. In addition to the edge structure, Basko et al. point out that x-ray fluoresence lines should be efficiently excited for the heavier elements, and that this effect should be quite substantial for Fe. The wavelength of the α KL line of Fe will depend on the stage of ionization of the ion which is excited, and will vary from ~ 6.40 keV (1.936Å) [110] for Fe I to 6.70 keV (1.867Å) for Fe XXV [111]. Basko et al. predict that the intensity in this feature should exceed the intensity in the primary continuum over a range of ~ 100 eV (i.e. equivalent width ~ 100 eV). Serlemitsos, Bolt, Holt, Rothschild and Saba [112] and Sanford, Mason and Ives [113] have observed a feature in Cyg X-3 at 6.7 keV which may be due to this phenomena, however alternate explanations may also be possible (see Section IV.B.3).

IV.B.2 SPECTRUM OF THE EXTENDED PHOTOIONIZED ATMOSPHERE

A number of authors [42,114,115] have discussed the interaction of the primary x-ray flux from a binary source with the surrounding material, which may be in the form of a stellar wind from the normal companion star, and with the surrounding ISM. Buff and McCray [116] and McCray [117] have discussed the structure, opacity, and emission spectrum of the photoionized atmosphere created in depth. If the accretion gas flow in the binary system is in the form of a stellar wind, a photoionized Strömgren sphere will be created around the x-ray source. The existence of this ionization zone has several important consequences for the spectrum of the source; the x-ray opacity of the surrounding material, and the consequent spectral features caused by internal absorption may become variable, and the photoionized atmosphere will itself emit a spectrum which may become observable. The effects of the atmosphere on the emergent x-ray spectrum are illustrated in Figure 9. The spectrum will, of course, be further altered by absorption in the ISM. Observations of Cygnus X-1 by the Copernicus satellite [118] have found a variable low energy cutoff which may be due to the effect predicted by Figure 9.

The ionization equilibrium created by a x-ray heated gas will result in a higher degree of ionization at a given electron temperature than in a gas in which the ionization is controlled by collision [117]. This ionization structure will result in an emission spectrum which is dominated by recombination processes. McCray has calculated the emission spectrum for an x-ray source of luminosity $L_x = 10^{37}$ ergs/sec, embedded in a stellar wind with density $n = 10^{12}$ cm^3. The strengths in a number of spectral features are given in Table IX. If such a source

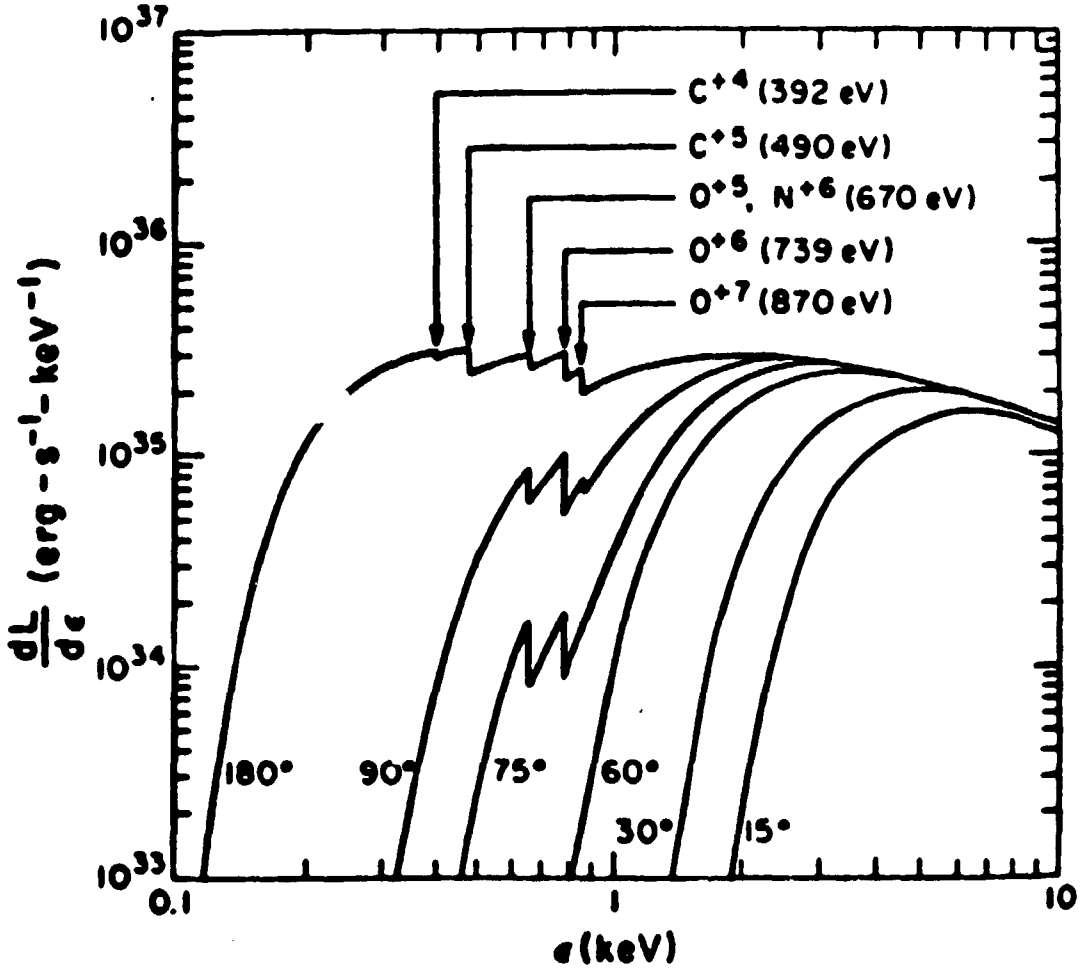

Fig. 9. Emergent x-ray spectrum for a x-ray source embedded in a stellar wind. The angle α is the angle at the x-ray source between the companion star and the direction of observation. (After Buff and McCray, Ref. 116)

TABLE IX

EMERGENT LUMINOSITIES IN VARIOUS LINES AND RECOMBINATION CONTINUA

Line		Luminosity erg s^{-1}	Recombination Edges		Luminosity erg s^{-1}
Lyman-α	1216	7.7×10^{34}	H I	912	2.7×10^{33}
Hα	6562	4.0×10^{33}	C VII	490 eV	4.1×10^{33}
He II	4686	3.2×10^{32}	N VIII	666 eV	1.2×10^{31}
C IV	1549	6.3×10^{34}	O IX	870 eV	9.6×10^{32}
N V	1238	6.0×10^{33}			
O VI	1035	4.0×10^{34}			
He II	40.8 eV	1.4×10^{35}			
C VI	367 eV	4.0×10^{33}			
O VIII	652 eV	9.8×10^{30}			

(After McCray, Ref. 117)

were not so distant that the soft x-ray features were too strongly attenuated by the ISM, a number of the features predicted by McCray should be sufficiently intense to be observable.

IV.B.3 OBSERVATIONS OF SPECTRAL STRUCTURE IN COMPACT X-RAY SOURCES

A number of attempts to observe the weak line cores expected in the spectrum of Sco X-1 have been carried out [119,120,121] using Bragg crystal spectrometers. These observations have, so far, proved unsuccessful, but have established upper limits which are close to the fluxes predicted by Felten et al. [106] for the Fe XXV intercombination and forbidden lines. An upper limit for the equivalent width of these lines of 25 eV has been established [121]. However, if the effects discussed by Mészáros [107] are important in Sco X-1, the line core might be spread over an energy band of $\sim$ 100-200 eV, so that the continuum to line ratio could be as large as 10-20 to 1, making the detection of the line extremely difficult with an instrument having a narrow bandwidth.

The only spectral feature definitely established for a binary source is the feature observed near 6.7 keV in Cyg X-3 by Serlemitsos et al. [112]. This feature has also been observed by the UK5 satellite [113]. A critical question in the identification of the source of this feature is the wavelength of the observed feature, which will allow the range of stages of ionization of Fe in which the feature is excited to be determined. House [122] has calculated the wavelength of the Kα line for all stages of ionization of Fe. If the energy of the feature is as high as $\sim$ 6.7 keV, this implies that the radiation is excited in a very high stage of ionization of Fe, $\sim$ Fe XXII-XXV. Models of the x-ray heated atmosphere of a normal star in a close x-ray binary system by Milgrom

and Salpeter [109] suggest that temperatures in excess of 10^7 °K will be generated in the illuminated atmosphere, so it appear quite feasible that absorption may occur in material in which the Fe is in a high stage of ionization.

An alternate explanation of the observed feature could be in the photoionized atmosphere discussed by McCray, however it appears unlikely that the atmosphere would have a sufficiently large optical depth to efficiently convert the hard intrinsic spectrum into fluorescent Fe Kα line photons.

IV.B.4 ANALYTICAL TECHNIQUES FOR THE STUDY OF COMPACT X-RAY SOURCES

The strongest spectral features observable in compact x-ray sources will be associated with the photoionized atmospheres which have been predicted to be an important feature of those binary sources which are powered by accretion from a stellar wind [116], and with fluorescent effects in the atmosphere of the normal star which will be heated to temperatures of several million degrees by the absorption of part of the x-ray flux from its condensed accreting companion [108,109]. In both cases, emission lines and recombination edges should be prominent features of the spectrum. The diagnostic techniques discussed in Section II should allow models of the density, temperature, and composition of the photoionized stellar wind, and of the x-ray heated atmosphere of the normal companion to be developed. The higher densities which are to be expected in these systems may allow the direct determination of density by the observation of the diagnostic x-ray line ratios given in Table II, in contrast to the situation in the solar corona where only upper limits have been obtained so far. However, the high degree of ionization caused by the intrinsic x-ray spectrum will result in a large ionization zone

in which the ions of the most abundant light elements (C,N,O,Ne) are completely stripped, so that only transitions in the hydrogenic ion, induced by radiative recombination, will be observable. The density diagnostic techniques discussed in Table II will not be useful in these regions of the stellar wind. However, the population of the 2^2S level, which is de-excited by two photon decay, will become density sensitive at densities which may be attained in the accretion disk and surrounding stellar wind. The critical density for the process

$$2s\ ^2S + e \rightarrow 2p\ ^2P \rightarrow 1s\ ^2S + h\nu$$

is $\sim 10^{12}$ cm^{-3} in C VI, $\sim 4 \times 10^{12}$ cm^{-3} in N VII and $\sim 10^{14}$ in O VIII [123]. The relative intensity Lymanα/Lymanβ may, therefore, become density sensitive for these ions. The relative intensity of the $3\ ^3P_2 - 2\ ^1S_0$ and $3\ ^2P_1 - 2\ ^1S_0$ transitions near 17Å in Fe XVII (see Table II) may also prove to be a useful diagnostic tool for compact x-ray sources.

IV.C CORONAE OF NORMAL STARS

Recently, the observation of two of the brightest stars in the sky, Sirius (α C.Ma) and Capella (α Aur) in soft x-rays has been reported [124-127]. A number of authors have predicted soft fluxes for nearby stars [128-132] which have suggested that a number of objects can be studied in detail with suitable instrumentation. Recent ultraviolet observations have also resulted in the detection of stellar chromospheres and coronae, which imply the existence of measurable soft x-ray fluxes for a number of nearby stars [133-140]. The ultraviolet observations are summarized in Table X. Several nearby stars which have nearly solar type spectra, and which might have x-ray luminosity much like the solar x-ray luminosity, are also included in the listing.

TABLE X

MODELS OF STELLAR CORONAE AND CHROMOSPHERES

Star	Distance pc	Spectrum	Observation	Comment	Reference
α Cen	1.3	G2 V		Solar Type Spectrum	
α C.Mi (Procyon)	3.5	F5 IV-V	Si III $\lambda\lambda$1206 Mg II $\lambda\lambda$2796 O VI $\lambda\lambda$1032	$T_{corona} > 5 \times 10^5$ °K Chromospheric Line	Evans et al. [133,138] Ayres et al. [136]
σ Pav	5.7	G6 V		Solar Type Spectrum	
η Cas	5.9	G0 V		Solar Type Spectrum	
82 Eri	6.2	G5 V		Solar Type Spectrum	
β Hyi	6.3	G1 IV		Solar Type Spectrum	
β Gem (Pollux)	10.7	K0 III	O V $\lambda\lambda$1218	$T_{corona} \sim 2 \times 10^5$	Gerola et al.[134] McClintock et al.[135]
α Boo (Arcturua)	11.1	K2 III	Mg II $\lambda\lambda$2796	Chromospheric Line	Moos et al. [139] McClintock et al.[135]
α Aur (Capella)	14.0	G5 III/G0 III	O VI $\lambda\lambda$1032	Coronal Line	Dupree [137]
α Tau	20.3	K5 III	Mg II $\lambda\lambda$2796	Chromospheric Line	McClintock et al.[135]

The models developed from the uv observations listed in Table X are not, however, sufficiently well developed to predict fluxes at soft x-ray wavelengths. The model of Landini and Fossi [131] predicts quite large fluxes at the earth in the 44-60Å band for a number of stars; i.e. ~ 1 photon/cm^{2}sec ($\sim 10^{-9}$ ergs/cm^2/sec) for α C.Mi. A more conservative estimate can be obtained by computing the observed solar flux at the distance of α Centauri, which is close to the sun in spectral type. The derived soft x-ray fluxes are shown in Table XI [141].

IV.C.1 X-RAY OBSERVATIONS

A number of observational surveys of normal stars at soft x-ray wavelengths have recently been reported [127,142,143]. These surveys have reported negative results for $\sim 70 - 80$ stars. Margon et al. observed four nearby red giants (ϵ Sco, γ Dra, θ Cen, and α Boo) in the wavelength band ~ 10 to ~ 100Å. The upper limits found were $\sim 1\text{-}3 \times 10^{-9}$ ergs/cm^2/sec, corresponding to $L_x/L \leq 8 \times 10^{-5}$ for this class of object. Vanderhill et al. observed approximately 50 stars in the energy range between near 0.26 keV, with a sensitivity ~ 0.6 photons/cm^2/sec keV. Mewe et al. [127] have also carried out observations near 0.26 keV for ~ 25 stars, without positive results. In most cases, however, the upper limits established do not preclude that the stars observed are x-ray sources with the same efficiency as the sun, $L_x/L \sim 2 \times 10^{-6}$ in the energy band 0.2-0.28 keV.

Catura et al. [124] and Mewe et al. [125-127] have reported the positive identification of soft x-rays from Sirius (α C.Mi) and Capella (α Aur). The flux reported for Capella by Catura et al. corresponds to an x-ray luminosity of $L_x \leq 10^{31}$ ergs/sec. Mewe et al. [127] have also observed Capella, obtaining a flux of $L_x \sim 2\text{-}3 \times 10^{29}$ ergs/sec in the 0.2-0.284 keV band, and $\sim 10^{28}$ ergs/sec for Sirius.

TABLE XVI

PREDICTED SOFT X-RAY FLUXES FOR α CEN

(Å)	F_0*	G2V F(star at 1.3 pc) (no absorption)
0 - 10	2-100 x 10^{5}†	3-140 x 10^{-6}
10 - 20	8-40 x 10^{6}†	1.1-5.5 x 10^{-4}
20 - 30	8-40 x 10^{6}†	1.1-5.5 x 10^{-4}
40 - 50	4.0 x 10^{7}*	5.6 x 10^{-4}
50 - 60	7.6 x 10^{7}*	1.1 x 10^{-3}
60 - 70	8.7 x 10^{7}*	1.2 x 10^{-3}
70 - 80	8.3 x 10^{7}*	1.2 x 10^{-3}
80 - 90	1.1 x 10^{8}*	1.5 x 10^{-3}
90 - 100	1.0 x 10^{8}*	1.4 x 10^{-3}
100 - 110	6.1 x 10^{7}*	8.5 x 10^{-4}
110 - 120	3.2 x 10^{7}*	4.4 x 10^{-4}
120 - 130	1.3 x 10^{7}*	1.8 x 10^{-4}
SUM (40 - 130)	6 x 10^{8}	8.4 x 10^{-2}

(After Withbroe, Ref. 141)

*Solar flux at 1 AU (Manson, Ref. 32) photons/cm^2/sec

†Solar flux at 1 AU (Walker et al., Refs. 7,11)

Both Capella and Sirius are binaries, Capella containing G5 III and GO III giants, and Sirius an Al V main sequence star and a white dwarf. There is strong evidence that at least Capella is a strongly variable source. Mewe et al. suggest that the soft x-ray emission in this object may arise from a high temperature coronae in the primary of this system, with a coronal temperature not greatly different from the solar coronal temperature. This conclusion is strongly reinforced by the ultraviolet observations of Dupree [137]. In the case of Sirius, Mewe et al. present arguments which suggest that the x-ray emission comes not from the primary, but rather from the white dwarf companion.

IV.C.2 ANALYTICAL TECHNIQUES

It appears probable from the models derived [133,135,137] on the basis of the presently available observations, that stellar corona will have temperature and density profiles which are within an order of magnitude of the corresponding solar values. Consequently, the diagnostic observations discussed in Section II should prove useful for these sources, provided instrumentation of suitably large aperture can be developed to make the flux in individual lines observable. Initial observations are likely to be confined to broad band instruments, or at best to techniques, such as Ross Filters [144], which isolate narrow bands containing several spectral lines and continuum. Theoretical spectral models will be required to interpret these observations, and the techniques described in Section II must be modified for these lower resolution observations.

IV.D DIFFUSE GALACTIC SOURCES

We have already discussed the observation of the ISM by the study of the effects of the ISM opacity on the x-ray spectra of cosmic sources. Recent observations of extended soft emission features by Williamson et al. [72] have suggested that portions of the ISM are at temperatures in excess of 3×10^5 ^oK, and are detectable as emission features at soft x-ray wavelengths. A detailed account of these observations is given elsewhere in these proceedings [145].

IV.D.1 THEORETICAL PREDICTIONS AND OBSERVATIONS

There has accumulated, by various observational techniques, a body of evidence which suggests that the galaxy possesses a gaseous halo (or galactic wind if the halo is in fact escaping from the galaxy). Silk [146] has discussed these observations, and in particular the diffuse galactic radio and soft x-ray emission at high latitudes, and suggests that they are consistent with a diffuse galactic halo with temperature $\sim$ 1-2 $\times 10^6$ ^oK, radius 10 kpc, and electron density $\sim 10^{-3} cm^{-3}$. A number of authors [147,148,73,74] have suggested that the remnants of old supernovae may evolve into large fossil Strömgren spheres, the Gum Nebula being a prototype of the class of object postulated, and may account for the diffuse high latitude emission at radio and soft x-ray wavelengths. These objects were first observed as galactic spurs or loops at radio wavelengths [149], and later one object, the North Polar Spur (or Loop I) was observed as a diffuse soft x-ray source [150].

Cox and Smith [81] and Chevalier [82] have suggested that the zones of hot ionized low density gas created by supernovae explosions may

eventually interconnect, creating tunnels of low density hot interstellar material which co-exist with the intercloud medium discussed in Section III. New supernovae could supply energy to maintain the network. The parameters of this network of tunnels predicted by Cox and Smith are $3 \times 10^5\ ^oK < T < 1 \times 10^6\ ^oK$ and $n_e \sim 3 \times 10^{-3}\ cm^{-3}$. Cox and Smith suggest that a substantial fraction of the volume in the ISM may be occupied by such regions. The theories put forward by Cox and Smith and Chevalier appear to offer an attractive explanation of these phenomena, and might offer a source for the creation of a galactic halo as discussed by Silk [146].

The observations of Williamson et al. [72] have mapped three extensive regions of enhanced soft x-ray emission. Williamson et al. have also reviewed earlier observations of enhanced soft x-ray emission. These observations suggest many individual regions of hot interstellar gas, since the very soft spectrum of the observed emission is inconsistent with a single distant source.

IV.D.2 ANALYTICAL TECHNIQUES

The x-ray observations [72] suggest that the observed diffuse soft emission is due to thermal emission from material with near solar abundances, and with temperature $T \sim 3\text{-}20 \times 10^5\ ^oK$ and density $\sim 10^{-3}/cm^3$. The flux from a plasma with these parameters will consist of $\sim 90\%$ line emission, and will resemble the spectrum from the solar corona and transition region. Many of the diagnostic techniques discussed in Section II for the development of models of temperature structure, ionization structure, and composition should prove useful in the study of these regions in the ISM. Borken [145] has discussed an observational program intended to obtain high resolution spectra of these regions.

IV.E OTHER GALACTIC SOURCES

We have identified four classes of observed galactic x-ray sources, and although only two stellar coronae have so far been observed, improved sensitivity appears likely to significantly increase the number of observable sources in all four categories. In this section, we discuss three additional classes of objects which have been predicted to be emitters of soft x-ray or euv, the flar stars, uv stars, and interstellar shocks associated with early type stars. Objects of all three classes might be expected to contain strong emission lines in their spectra.

IV.E.1 FLARE STARS

The star UV Ceti (L726-8AB) is the prototype of a class of faint low mass dwarfs in the solar neighborhood which are characterized by giant radio and optical flares. A number of authors [151-154] have predicted soft x-ray fluxes for these flares, based on various scaling laws for solar flares. Observations with the ANS satellite by Heise et al. [155] have now found x-rays correlated, in the cases where simultaneous data was available, with optical flares in UV Ceti and Ross 882[YZ C.Mi]. The peak flux from Ross 882 corresponds to a peak luminosity of 3.6×10^{30} ergs/sec. The peak flux from the UV Ceti event was found to be $\sim 6 \times 10^{28}$ ergs/sec. The duration of the Ross 882 event was ~ 6 minutes, and of the UV Ceti event ~ 1 minute. Several observed UV Ceti optical flares were not correlated with observable x-ray events. The soft x-ray flux observed from UV Ceti was below all of the scaling predictions based on the intensity of the observed optical flare. Heise et al. conclude that if the UV Ceti flare observed is reasonably

typical for this class of object, the contribution of flare stars to the total soft x-ray background is small, but if the more intense Ross 882 event is typical, the total soft x-ray background contributed by flare stars could be significant.

IV.E.2 UV STARS

Hills [156] has discussed the spectra of hot pre-white dwarfs, and the nuclei of planetary nebulae, which he has called UV stars. These objects are known to have temperatures in excess of 10^5 °K [157,158] and should be intense uv sources down to wavelengths shortward of 200Å. This is a second class of stellar object which may be observable at euv wavelengths. Predictions of expected fluxes are given by Henry [158] and the references therein. Withbroe [141] has discussed three of the closest candidate stars; these objects are listed in Table XII.

TABLE XII

NEARBY "UV" STARS

Star	Spectra	Distance	Estimated Temperature °K
Hz 21	DO	60 pc	10^5
G191B2B	DA wk	20 pc	10^5
Hz 43	DA wk	30 pc	5×10^4

(After Withbroe, Ref. 141)

IV.E.3 EARLY TYPE STARS

The Copernicus satellite has detected OVI λλ1032;1038 interstellar absorption lines in the spectra of ~ 30 early type stars [159,160]. Other lines of highly ionized elements (C III, C IV, N II, N V, Si IV) have also been observed, and temperature limits 2×10^5 °K < T < 2×10^6 °K have been placed on the regions observed. Castor, McCray and Weaver [161]

have suggested that the Copernicus observations can be explained by "interstellar bubbles", consisting of shocks due to the interaction of the strong stellar wind of early type stars with the ISM. The calculations of Castor et al. predict temperatures $T \approx 10^6$ °K and densities $n \approx 0.01$ cm^{-3}. An alternate explanation of the Copernicus observations is the interconnecting supernovae remnants predicted by Cox and Smith [73] and Chevalier [74]. Both models would, however, predict that a thermal soft x-ray emission spectrum, dominated by lines, should be associated with the material responsible for the absorption lines observed by Copernicus.

IV.F EXTRAGALACTIC SOURCES

Kellog [162] has reviewed the observations of extragalactic sources. Approximately 30 sources have been identified with extragalactic objects, and there are an equal number of unidentified Uhuru sources at high galactic latitudes which might be of extragalactic nature.* We are concerned here with the largest class of extragalactic sources, the Cluster x-ray sources. These objects have an optically thin spectrum, and spectroscopic observations may well prove decisive in investigating their nature and evolution.

IV.F.1 THE CLUSTER X-RAY SOURCES

The cluster x-ray sources are extended sources which are associated with large clusters of galaxies. The brightest of these sources have luminosities of $\sim$ 3-5 x 10^{44} ergs/sec, dimensions of megaparsecs, and contain hundreds of luminous galaxies, and thousands of less luminous

*Some of these objects have recently been identified with x-ray binaries in globular clusters by the MIT group [167].

galaxies. The spectra of these sources has been found to be compatible with a thermal bremsstrahlung spectrum for the brightest objects by Lea et al. [163] and Gorenstein et al. [164], with temperatures $T \sim 9.5 \times 10^7$ °K for the Coma cluster and $T \sim 8.8 \times 10^7$ °K for the Perseus cluster. Kellog [162] points out that the spectra of these objects is also consistent with the inverse Compton effect [165]. However, we explore here only the implications of a thermal model of the emission.

If the gas responsible for the cluster sources is primordial then the abundance of heavy elements will be very low, and no emission features will be observed at x-ray wavelengths. However, if the gas originates from one or more of the member galaxies, it might have cosmic abundances, and line emission due to recombination to hydrogenic ions might be observable. Since the cluster sources are not strongly cutoff at low energies, the Lyman α lines of a number of elements (Fe, Ne, O, C) might be detected. The search for such structure in the spectra of cluster sources might prove decisive in determining the origin of the intracluster gas.

V. CONCLUSIONS

In the preceding paper we have reviewed the spectroscopic observations and analytical techniques which have been used in the study of the solar corona, and briefly discussed modifications of these techniques which may be required in the study of non-solar sources. The techniques discussed include the general analytical approach for the development of thermal models of an optically thin source, and diagnostic techniques for the study of temperature, density, composition, and ionization equilibrium, which may be used when sufficient data is not available to develop a complete thermal model.

Two programs of spectroscopic observations of non-solar x-ray sources were then presented; the study of the properties of the ISM by measurements of the x-ray opacity of the ISM, and the spectroscopic study of individual sources. The present knowledge of the opacity of the ISM was reviewed in depth; the excellent prospects for obtaining unique information on total ISM abundances, ionization structure, and grain size and composition were pointed out.

The expected spectroscopic characteristics of seven classes of x-ray sources are discussed, and the development of models for source parameters with spectroscopic observations briefly reviewed. For supernovae remnants, the spectra are optically thin, and should contain strong line emission. The determination of thermal models, abundances, and the study of the ionization equilibrium of these objects should prove feasible with the development of x-ray spectroscopic observatories.

The spectra of the binary x-ray sources will be more complex, consisting of at least four components; an optically thick intrinsic

spectrum containing weak line cores substantially broadened by a number of processes; emission from the x-ray heated outer atmosphere of the normal companion of the x-ray emitting condensed star, an emission spectrum from the photoionized stellar wind which may be the source of the accreted material in many x-ray binaries; and variable absorption profiles which are caused by the opacity of the stellar wind. The last three components of the spectrum are likely to contain strong spectral features, which can be interpreted to develop models of the temperature, density, composition and ionization structure of the extended atmosphere of the binary source. Many of the analytical techniques developed in solar x-ray studies will be useful in the study of these objects.

Two normal binary stars have now been detected as soft x-ray sources, and in at least one case (Capella), there is strong evidence that the emission comes from a stellar corona. Recent ultraviolet observations of chromospheric and transition region lines, and in one case (β Gem) of a coronal line, reinforce the predictions that many late type stars will be found to have x-ray emitting coronae. The low values found for the local ISM density ($n_H \sim 0.01\text{-}0.10$ cm^{-3}) make the prospects for the study of stellar coronae in the neighborhood of the sun at soft x-ray and euv wavelengths most promising. Many of the diagnostic techniques developed for the study of the solar corona should prove useful for these objects.

The existence of regions in the ISM where the temperature is $\sim 3 \times 10^5 - 2 \times 10^6$ ^oK, and densities are $1\text{-}3 \times 10^{-3}$ cm^{-3} has now been demonstrated by the observation of their emission in soft x-rays. These regions may occupy a significant volume within the ISM, and may be related

to a hot galactic halo. Their existence may be related to the fossil Strömgren spheres created by galactic supernovae remnants. These regions will have a strong emission line spectrum, and their analysis should be able to make use of many of the previously discussed diagnostic techniques.

Two other types of galactic soft x-ray and euv sources have been extensively discussed in the literature, flare stars and uv stars. Transient soft x-ray emission has now been detected from two flare stars, however emission from uv stars in the euv has not yet been reported. Both types of source should have spectra containing strong emission features. More recently, it has been suggested that the stellar winds of early type stars may create hot ($T \sim 10^6$ ^oK) low density bubbles in the ISM which might have emission properties similar to evolved supernovae remnants.

The most interesting class of extragalactic source spectroscopically is the cluster x-ray sources associated with large clusters of galaxies. These sources are highly luminous ($\sim 10^{44}$ ergs/sec) and of enormous extent ($\sim 10^5$ - 10^6 parsecs) and so are optically thin. If these sources are thermal, and thermal models are able to explain the presently available observations, the search for emission lines of hydrogenic ions due to recombination processes will be important to the resolution of competing models of the source of the hot intergalactic gas which is responsible for the emission.

Because of the weakness of cosmic x-ray sources, spectroscopic observations have been undertaken for only a few objects, and only one spectroscopic feature has been definitely identified (in the binary system Cyg X-3). However, with sufficiently powerful instrumentation a large number of spectral features will become observable in every class

of known x-ray object. Many of the diagnostic and analytical tools required to interpret these observations in the development of source models are already available as a result of studies of the solar corona. Because all of the sources discussed will have either weak broad spectral features (such as line cores or absorption or emission edges) or a multiplicity of spectral features (such as emission lines in supernovae interstellar shocks or stellar coronae) instruments which combine high throughput with good spectral resolution will be required. The recent significant improvements in soft x-ray gratings discussed later in these proceedings [166] should prove of immense significance for the spectroscopy of cosmic x-ray sources.

The author would like to thank a number of authors who allowed access to unpublished manuscripts and preprints, especially Drs. G. L. Withbroe and A. K. Dupree of HCO, and Dr. J. Linsky and J. Castor of JILA. The work reported in this paper has been supported by the National Aeronautics and Space Administration under Grants NSG-7099 and NSG-2049.

REFERENCES

1. Pottasch, S. R.: Sp. Sci. Rev., 3, 816 (1964).

2. _____.: Bull. Astron. Inst. Neth., 19, 113 (1967).

3. Gabriel, A. H. and Jordan, C.: Case Studies in Atomic Collision Physics, Vol. II, Eds. E. W. McDaniel and M. R. C. McDowell, North Holland Publishing Co., Amsterdam, Holland, 1972, p. 211.

4. Walker, A. B. C. Jr.: Sp. Sci. Rev., 13, 672 (1972).

5. _____.: Solar Gamma, X and EUV Radiation, Proceedings of IAU Symp. No. 68, Buenos Aires, Argentina, Ed. S. R. Kane, D. Reidel Publishing Co., Dordrecht, Holland, 1975, p. 73.

6. Jefferies, J. T., Orrall, G. Q., and Zirker, J. B.: Sol. Phys., 22, 307 (1972).
   _____.: ibid, 22, 317 (1972).
   _____.: ibid, 22, 327 (1972).

7. Walker, A. B. C. Jr., Rugge, H. R., and Weiss, K.: Astrophys. J., 188, 423 (1974).

8. Chambre, G.: Astron. Astrophys., 12, 210 (1971).

9. Acton, L. W., Catura, R. C., Meyerott, A. J., Wolfson, C. J., and Culhane, J. L.: Sol. Phys., 26, 183 (1972).

10. Batstone, R. M., Evans, K., Parkinson, J. H., and Pounds, K. A.: Sol. Phys., 13, 389 (1970).

11. Walker, A. B. C. Jr., Rugge, H. R., and Weiss, K.: Astrophys. J., 192, 169 (1974).
    _____.: ibid, 194, 471 (1974).

12. Phillips, K. J. H.: Astrophys. J., 199, 247 (1975).

13. Parkinson, J. H.: Sol. Phys., 42, 183 (1975).

14. Dupree, A. K.: Astrophys. J., 178, 527 (1972).

15. Kopp, R. A.: Sol. Phys., 27, 393 (1972).

16. Pneuman, G. W.: Astrophys. J., 177, 793 (1972).

17. Jordan, C.: Solar Gamma, X and EUV Radiation, Proceedings of IAU Symp. No. 68, Buenos Aires, Argentina, Ed. S. R. Kane, D. Reidel Publishing Co., Dordrecht, Holland, 1975, p. 109.

Jordan, C.: Paper presented at the Royal Society Discussion Meeting on the Physics of the Solar Atmosphere, January 1975, to be published in Phil. Trans. Roy. Soc. Lon.

18. Malinovsky, M. and Heroux, L.: Astrophys. J., 181, 1009 (1973).

19. Rugge, H. R. and Walker, A. B. C. Jr.: Astron. Astrophys., 33, 367 (1974).

20. Hutcheon, R. J. and McWhirter, R. W. P.: J. Phys. B, 6, 2268 (1973).

21. Gabriel, A. H.: Mon. Not. R. Astr. Soc., 160, 99 (1972).
Bhalla, C. P., Gabriel, A. H., and Presnyakov, L. P.: Mon. Not. R. Astr. Soc., 172, 359 (1975).

22. Parkinson, J. H.: Solar Gamma, X and EUV Radiation, Proceedings of IAU Symp. No. 68, Buenos Aires, Argentina, Ed. S. R. Kane, D. Reidel Publishing Co., Dordrecht, Holland, 1975, p. 45.

23. Walker, A. B. C. Jr. and Rugge, H. R.: Astrophys. J., 164, 181 (1971).

24. Gabriel, A. H. and Jordan, C.: Astrophys. J., 186, 327 (1973).

25. Mewe, R. and Schrijver, J.: to be published Sol. Phys. (1975).

26. Munro, R. H., Dupree, A. K., and Withbroe, G. L.: Sol. Phys., 19, 347 (1971).

27. Jordan, C.: Highlights in Astronomy, Ed. C. deJager, D. Reidel Publishing Co., Dordrecht, Holland, 1971, p. 519.

28. Malinovsky, M., Heroux, L., and Sahal Brechot, S.: Astron. Astrophys., 23, 291 (1973).

29. Donnelly, R. F. and Hall, L. A.: Sol. Phys., 31, 411 (1973).

30. Jordan, C.: Astron. Astrophys., 34, 69 (1974).

31. Loulergue, M. and Nussbaumer, H.: Astron. Astrophys., 34, 225 (1974).

32. Widing, K. G. and Sandlin, G. D.: Astrophys. J., 152, 545 (1968).
Freeman, F. F. and Jones, B. B.: Sol. Phys., 15, 298 (1970).
Manson, J. E.: Sol. Phys., 27, 107 (1972).
Behring, W. E., Cohen, L., and Feldman, U.: Astrophys. J., 175, 493 (1972).

33. Parkinson, J. H.: Astron. Astrophys., 24, 215 (1973).

34. Garstang, R. H.: Pub. A.S.P., 81, 488 (1969).

35. Acton, L. W., Catura, R. C., and Joki, E. G.: Astrophys. J. (Letters), 195, L93 (1975).

36. Rugge, H. R. and Walker, A. B. C. Jr.: submitted to Astrophys. J. (Letters) (1975).

37. Jordan, C.: Mon. Not. R. Astr. Soc., 142, 499 (1969).
_____.: ibid, 149, 1 (1970).

38. Landini, M. and Fossi, B. C.: Astron. Astrophys. Suppl., 7, 291 (1972).

39. Burgess, A. and Summers, H. P.: Astrophys. J., 157, 1007 (1969).

40. Summers, H. P.: Mon. Not. R. Astr. Soc., 158, 255 (1972).
_____.: ibid, 169, 663 (1974).

41. Kaftos, M. C. and Tucker, W. H.: Astrophys. J., 175, 837 (1972).

Landini, M., Fossi, B. C., and Pallavicini, R.: Sol. Phys., 29, 93 (1973).

42. Tarter, C. B., Tucker, W. H., and Salpeter, E. E.: Astrophys. J., 156, 943 (1969).

43. Tarter, C. B. and Salpeter, E. E.: Astrophys. J., 156, 953 (1969).

44. Cruddace, R., Paresce, F., Bowyer, S., and Lampton, M.: Astrophys. J., 187, 497 (1974).

45. Strom, S. E. and Strom, K. M.: Pub. A.S.P., 73, 43 (1960).

46. Pikel'ner, S. B.: Ann. Rev. Astron. Astrophys., 6, 165 (1968).

47. Seward, F. D., Burginyon, G. A., Grader, R. J., Hill, R. W., and Palmieri, T. M.: Astrophys. J., 178, 131 (1972).

48. Grewing, M., Lamero, H. J., Walmsley, C. M., and Wolfmathis, C.: Astron. Astrophys., 27, 115 (1973).

49. Felten, J. E. and Gould, R. J.: Phys. Rev. Letts., 17, 401 (1966).

50. Bell, K. L. and Kingston, A. E.: Mon. Not. R. Astr. Soc., 136, 241 (1967).

51. Brown, R. L. and Gould, R. J.: Phys. Rev., D1, 2251 (1970).

52. Brown, R. L.: Astrophys. Sp. Sci., 18, 329 (1972).

53. Martin, P. G.: Mon. Not. R. Astr. Soc., 149, 221 (1970).

54. Overbeck, J. W.: Astrophys. J., 141, 864 (1965).

55. Hayakawa, S.: Prog. Theor. Phys., 43, 1224 (1970).

56. Martin, P. G. and Sciama, D. W.: Astrophys. Letts., 5, 193 (1970).

57. Fireman, E. L.: Astrophys. J., 187, 57 (1974).

58. Ride, S. K. and Walker, A. B. C. Jr.: submitted to Astrophys. J. (1975).

59. Field, G. B.: Astrophysics and General Relativity, Eds. S. Desai and J. Goldstein, Gordon and Breach, New York, 1973, p. 61.

_____.: Molecules in the Galactic Environment, Eds. M. A. Gordon and L. E. Snyder, John Wiley and Sons, New York, 1973, p. 21.

60. Greenberg, J. M.: Astrophys. J. (Letters), 189, L81 (1974).

61. Field, G. B.: Astrophys. J., 187, 453 (1974).

62. Morton, D. C.: Astrophys. J., 197, 85 (1975).

63. Talbot, R. J.: Astrophys. J., 189, 209 (1974).

64. Charles, P. A., Culhane, J. L., and Tuohy, I. R.: Mon. Not. R. Astr. Soc., 165, 355 (1973).

65. Ride, S. K.: private communication.

66. Gorenstein, P.: Astrophys. J., 198, 95 (1975).

67. Ryter, C., Cesarsky, C., and Audouze, J.: Astrophys. J., 198, 103 (1975).

68. Bohland, R. C.: Astrophys. J., 182, 139 (1973).

_____.: to be submitted to Astrophys. J. (1975).

Fahr, H. J.: Sp. Sci. Rev., 15, 483 (1974).

Savage, B. D. and Jenkins, E. B.: Astrophys. J., 172, 491 (1972).

Jenkins, E. B. and Savage, B. D.: Astrophys. J., 187, 243 (1974).

Savage, B. D. and Panek, R. J.: Astrophys. J., 191, 659 (1974).

Rogerson, J. B. and York, D. G.: Astrophys. J. (Letters), 186, L95 (1973).

McClintock, W., Linsky, J. L., Henry, R. C., and Moos, H. W.: Astrophys. J. (in press) (1975).

_____.: preprint (1975).

69. Van der Kamp, P.: Ann. Rev. Astron. Astrophys., 9, 103 (1971).

Gliese, W.: Veröff Astron. Rechen-Inst., Heidelberg No. 22 (1969).

70. Giacconi, R. and Gursky, H. (Eds.): X-Ray Astronomy, D. Reidel Publishing Co., Dordrecht, Holland (1974).

71. Culhane, J. L.: Vistas in Astronomy, 19, 1 (1975).

_____.: "Some Recent Results in X-Ray Astronomy", Paper presented at the Second European Regional Meeting on Astronomy Trieste, 1974.

72. Williamson, F. O., Sanders, W. T., Kraushaar, W. L., McCammon, D., Borken, R., and Bunner, A. N.: Astrophys. J. (Letters), 193, L127 (1974).

73. Cox, D. P. and Smith, B. W.: Astrophys. J. (Letters), 189, L105 (1974).

74. Chevalier, R. A.: Astrophys. J., 188, 501 (1974).

75. Silk, J.: Ann. Rev. Astron. Astrophys., 11, 269 (1973).

76. Hills, J. G.: Astrophys. Letts., 14, 69 (1973).

77. Landini, M. and Fossi, B. C.: Astron. Astrophys., 25, 9 (1973).

78. Wolter, L.: Ann. Rev. Astron. Astrophys., 10, 129 (1972).

79. Shklovsky, I. S.: Supernovae, Nauka Moscow (1966). [Eng. Trans. Interscience, New York, 1968].

80. Tucker, W. H.: Astrophys. J. (Letters), 167, L85 (1970).

_____.: Astrophys. Sp. Sci., 9, 315 (1971).

81. Cox, D. P.: Astrophys. J., 178, 143, 159, 169 (1972).

82. Gorenstein, P., Harnden, F. R. Jr., and Tucker, W. H.: Astrophys. J., 192, 661 (1974).

83. Gorenstein, P. and Tucker, W. H.: X-Ray Astronomy, Eds. R. Giacconi and H. Gursky, D. Reidel Publishing Co., Dordrecht, Holland, 1974, p. 267.

84. Mansfield, V. N. and Salpeter, E. E.: Supernovae and Supernovae Remnants, Ed. C. B. Cosmovici, D. Reidel Publishing Co., Dordrecht, Holland, 1974, p. 251.

85. Straka, W. C. and Lada, C. J.: Astrophys. J., 195, 563 (1975).

86. McKee, C. F.: Astrophys. J., 188, 335 (1974).

87. Gull, S. F.: Mon. Not. R. Astr. Soc., 171, 263 (1975).

88. Ilovaisky, S. A. and Ryter, C.: Astron. Astrophys., 18, 163 (1972).

89. Zarnecki, J. C., Culhane, J. L., Fabian, A., Rapley, G., Silk, R., Parkinson, J. H., and Pounds, K.: Nature Phys. Sci., 243, 4 (1973).

90. Fabian, A. C., Zarnecki, J. C., and Culhane, J. L.: Nature Phys. Sci., 242, 18 (1973).

91. Charles, P. A., Culhane, J. L., and Zarnecki, J. C.: Astrophys. J. (Letters), 196, L19 (1975).

92. Burginyon, G. A., Hill, R. W., and Seward, F. D.: Astrophys. J., 200,

93. Tannenbaum, H. and Tucker, W. H.: X-Ray Astronomy, Eds. R. Giacconi and H. Gursky, D. Reidel Publishing Co., Dordrecht, Holland, 1974, p. 207.

94. Blumenthal, G. R. and Tucker, W. H.: Ann. Rev. Astron. Astrophys., 12, 23 (1974).

95. Prendergast, K. H. and Burbidge, G. R.: Astrophys. J. (Letters), 151, L83 (1968).

96. Zel'dovich, Ya. B. and Novihov, I. D.: Relativistic Astrophysics, Nauka (1967). [Eng. Trans. University of Chicago, Press, Chicago, 1971].

97. Pringle, J. E. and Rees, M. J.: Astron. Astrophys., 21, 1 (1972).

98. Alme, M. L. and Wilson, J. R.: Astrophys. J., 186, 1015 (1973).

99. Shakura, N. I. and Sunyaev, R. A.: Astron. Astrophys., 24, 337 (1973).

100. Shakura, N. I.: Astron. Zhurnal, 49, 521 (1972). [Eng. Trans. Soviet Astron., 16, 756 (1973)].

101. Davidson, K. and Ostriker, J. P.: Astrophys. J., 179, 585 (1973).

102. Lamb, F. K., Pethick, C. J., and Pines, D.: Astrophys. J., 184, 271 (1973).

103. Davidson, K.: Nature Phys. Sci., 246, 1 (1973).

104. Lamb, F. K.: Proceedings of the International Conference on X-Rays In Space, University of Calgary, Calgary, 1975, p. 613.

105. Felten, J. E. and Rees, M. J.: Astron. Astrophys., 17, 226 (1972).

106. Felten, J. E., Rees, M. J., and Adams, T. F.: Astron. Astrophys., 21, 139 (1972).

107. Mészáros, P.: Astron. Astrophys., 35, 171 (1974).

108. Basko, M. M., Sunyaev, R. A., and Titarchuk, L. G.: Astron. Astrophys., 31, 349 (1974).

109. Milgrom, M. and Salpeter, E. E.: Astrophys. J., 196, 583 (1973).
_____.: ibid, 196, 589 (1973).

110. Bearden, J. A.: Rev. Mod. Phys., 39, 78 (1967).

111. Ermolaev, A. M. and Jones, M.: J. Phys. B, 7, 199 (1974).

112. Serlemitsos, P. J., Bolt, E. A., Holt, S. S., Rothschild, R. E., and Saba, J. L. R.: "Spectral Variability of Cyg X-3", Goddard Space Flight Center Preprint (1975).

113. Sanford, P., Mason, K. O., and Ives, J.: "Observation of a Line Feature in the X-Ray Spectrum of Cygnus X-3", Mullard Space Science Laboratory Preprint (1975).

114. Silk, J., Goldsmith, D. W., Field, G. B., and Carraso, L.: Astron. Astrophys., 20, 287 (1972).

115. Hayakawa, S. and Tanaka, Y.: Astrophys. J. (Letters), 183, L5 (1973).

116. Buff, J. and McCray, R.: Astrophys. J. (Letters), 188, L37 (1974).
_____.: Astrophys. J., 189, 155 (1974).

117. McCray, R.: Proceedings of the International Conference on X-Rays in Space, University of Calgary, Calgary, 1975, p. 547.

118. Mason, K. O., Hawkins, F. J., Sanford, P. W., Murdin, P., and Savage, A.: Astrophys. J. (Letters), 192, L65 (1974).

119. Griffiths, R. E., Cooke, B. A., and Pounds, K. A.: Nature Phys. Sci., 229, 175 (1971).
_____.: ibid, 231, 136 (1971).

120. Keslenbaum, H., Angel, J. R. P., and Novick, R.: Astrophys. J. (Letters), 164, L87 (1971).

121. Griffiths, R. E.: Astron. Astrophys., 21, 97 (1972).

122. House, L. L.: Astrophys. J. Suppl., 18, 21 (1969).

123. Smith, T. S.: Les Transitions Interditesdans Les Spectres des Astres, Les Congre et Colloques de L'Université de Liege, Vol. 154, University of Liege, Belgium, 1969, p. 243.

124. Catura, R. C., Acton, L. W., and Johnson, H. M.: Astrophys. J. (Letters), 196, L47 (1975).

125. Mewe, R., Heise, J., Gronenschild, E.H.B.M., Brinkman, A. C., Schrijver, J., and den Boggende, A.J.F.: Laboratorium Voor Ruimteonderzoek Reprint No. 84, Utrecht [submitted to Nature Phys. Sci.] (1975).

126. Mewe, R., Heise, J., Gronenschild, E.H.B.M., Brinkman, A. C., Schrijver, J., and den Boggende, A.J.F.: Laboratorium Voor Ruimteonderzoek Reprint No. 87, Utrecht [submitted to Astrophys. Sp. Sci.] (1975).

127. _____.: ibid, Reprint No. 90 [submitted to Astrophys. J. (Letters)] (1975).

128. Biermann, L.: Proc. Roy. Soc. Lond. A, 313, 57 (1969).

129. de Lorre, C.: Astrophys. Sp. Sci., 6, 60 (1970).

130. de Jager, C. and de Lorre, C.: Non Solar X and Gamma Ray Astronomy, Ed. L. Gratton, D. Reidel Publishing Co., Dordrecht, Holland, 1970, p. 283.

131. Landini, M. and Fossi, B. C.: Astron. Astrophys., 25, 9 (1973).

132. Hills, J. G.: Astrophys. Letts., 14, 69 (1973).

133. Evans, R. G., Jordan, C., and Wilson, R.: Nature, 253, 612 (1975).

134. Gerola, H., Linsky, J. L., Shine, R. A., McClintock, W., Henry, R. C., and Moos, H. W.: Astrophys. J. (Letters), 193, L107 (1974).

135. McClintock, W., Linsky, J. L., Henry, R. C., and Moos, H. W.: Astrophys. J., in press (1975).

136. Ayres, T. R., Linsky, J. L., and Shine, R. A.: Astrophys. J., 192, 93 (1974).

137. Dupree, A. K.: Astrophys. J. (Letters), 200, L27 (1975).

138. Evans, R. G., Jordan, C., and Wilson, R.: Mon. Not. Roy. Astr. Soc., in press (1975).

139. Moos, W. H., Linsky, J. L., Henry, R. C., and McClintock, W.: Astrophys. J. (Letters), 188, L93 (1974).

Linsky, J. L.: "Late Type Stellar Chromospheres and Coronal Models and Copernicus Observations", Paper presented at IAU Colloquium No. 27, Cambridge, Mass., 1974.

140. Rogerson, J. B., York, D. G., Drake, J. F., Jenkins, E. B., Morton, L., and Spitzer, L.: Astrophys. J. (Letters), 181, L110 (1973).

York, D. G.: Astrophys. J. (Letters), 196, L103 (1975).

141. Withbroe, G. L.: private communication (1975).

142. Vanderhill, M. J., Borken, R. J., Bunner, A. N., Birstein, P. H., and Kraushaar, W. L.: Astrophys. J. (Letters), 197, L22 (1975).

143. Margon, B., Mason, K. O., and Sanford, P. W.: Astrophys. J. (Letters), 194, L75 (1974).

144. Ross, P. A.: J. Opt. Soc. Am., 16, 433 (1928).

145. Borken, R. J.: Proceedings of this Symposium (1975).

146. Silk, J.: Comments Astrophys. Sp. Phys., 6, 1 (1974).

147. Brandt, J. C. and Maran, S. P.: Nature, 235, 38 (1972).
_____.: ibid, 235, 348 (1972).

148. Kaftos, M. C. and Morrison, P.: Astron. Astrophys., 26, 71 (1973).

149. Haselam, C. G. T., Kahn, F. D., and Meaburn, J., Astron. Astrophys., 12, 388 (1971).

150. Bunner, A. N., Coleman, P. L., Kraushaar, W. L., and McCammon, D., Astrophys. J. (Letters), 172, L67 (1972).

151. Grindlay, J. E.: Astrophys. J., 162, 187 (1970).

152. Gurzadyan, G. A.: Astron. Astrophys., 13, 348 (1971).

153. Kahler, S. and Shulman, S.: Nature Phys. Sci., 237, 101 (1972).

154. Crannell, C. J., McClintock, J. E., and Moffett, T. J.: Nature, 252, 659 (1974).

155. Heise, J., Brinkman, A. C., Schrijver, J., Mewe, R., Gronenschild, E.H.B.M., den Broggende, A.J.F., and Gindlay, J.: Laboratorium Voor Reuimteonderzoek Reprint No. 89, Utrecht (1975).

156. Hills, J. G.: Astron. Astrophys., 12, 1 (1971).
_____.: ibid, 17, 55 (1972).
_____.: ibid, 26, 197 (1973).

157. Osterbrock, D. E.: Astrophysics of Gaseous Nebulae, W. H. Freeman and Co., San Francisco, 1974.

158. Henry,

159. Jenkins, E. B. and Meloy, D. A.: Astrophys. J. (Letters), 193, L121 (1974).

160. York, D. G.: Astrophys. J. (Letters), 193, L127 (1974).

161. Castor, J., McCray, R., and Weaver, R.: Astrophys. J., 200, , (1975).

162. Kellog, E. M.: X-Ray Astronomy, Eds. R. Giacconi and H. Gursky, D. Reidel Publishing Co., Dordrecht, Holland, 1974, p. 321.

163. Lea, S. M., Silk, J., Kellog, E. M., and Murray, S.: Astrophys. J. (Letters), 184, L105 (1973).

164. Gorenstein, P., Bjorkhorn, B., Harris, B., and Harnden, F.R.: Astrophys. J. (Letters), 183, L57 (1973).

165. Brown, R. L.: Astrophys. J. (Letters), 180, L49 (1973).

166. Steadman, M.: Proceedings of this Symposium (1975).

167. Clark, G. W., Market, T. H., and Li, F. K.: Astrophys. J. (Letters), 199, L93 (1975).

Canizares, C. R. and Neighbours, J. E.: Astrophys. J. (Letters), 199, L97 (1975).